Estimation Problems of Pollutant Emissions in Internal Combustion Engines

UNIVERSITÀ POLITECNICO DI BARI
DIPARTIMENTO DI INGEGNERIA ELETTRICA E DELL'INFORMAZIONE

DOCTORAL RESEARCH PROGRAM IN
ELECTRICAL AND INFORMATION ENGINEERING
CYCLE 33

Estimation Problems of Pollutant Emissions in Internal Combustion Engines

University supervisor: Prof. Paolo. Lino, Prof. Saverio Mascolo

PhD Candidate: Sama Molaie

ACADEMIC YEAR 2020

Table of Contents

ABSTRACT

This research deals with the question of how particulate matter (PM) from vehicle exhaust can be measured using low-cost and low-weight sensor and with high resolution. For this purpose, a novel system based on inexpensive commercial optical scattering-based sensor, ejectors, compressor, and filters is presented.

Atmospheric particulate matter poses a significant health hazard globally, which manifests itself in respiratory and cardiovascular disease and causes shortened life expectancy. As one source of pollution, diesel cars are equipped with a very efficient particulate matter filter to reduce the particulate matter emission from vehicle exhaust. However, any broken or removal of the particle filter can increase the vehicle 's PM emission by orders of magnitude. In order to recognize these high polluters, periodical emission measurement is suggested by regulations and manufacturers. The current regular tests have been assessed on the basis of data from high-cost, bulky and complex measurement devices. To this aim, the establishment of a new measurement sensor for periodic emission control and detection of the DPF performance after the vehicle exhaust is necessary.

To fulfill the requirements, this paper proposes the design of a new, simple, compact layout after the vehicle tailpipe based on the optical scattering-based sensor. Optical particle counters (OPCs) are widely used for real-time, mobile detection of the aerosol particles from a low concentration environment (e.g., clean room) to highly concentrated urban areas.

The proposed layout uses an optical particle counter as a compact instrument for real-time monitoring of the particle concentration after exhaust of the internal combustion engine. Various parameters of the exhaust emission before the optical sensor, such as temperature, humidity, and flow rate are considered to verify the working condition of the optical sensor.

Chapter 1:

Introduction of particulate matter, effects and control

1.1. Total overview of air pollution and environmental effect:

Air pollution has been a significant risk to human health and the environment. In 1970, the Clean Air Act (CAA) established the first regulation on National Ambient Air Quality Standards (NAAQS [1]). These emission standards set limits on six air pollutants that may be emitted from specific sources over specific timeframes: carbon monoxide, lead, nitrogen dioxide, ozone, sulfur dioxide, and particulate matter (PM)[2].

In particular, growing evidence from the last decade implicates effect of PM pollutants in increasing primary chronic diseases and the risk of premature mortality[3]. Besides, global healthcare maintenance costs are rapidly growing, while the increased daily risks from PM exposure remain modest for any individual. There is an exciting background of efforts to recognize the harmful outcomes of PM air pollution on human health and the environment. The research findings implicated the numerous harmful health effects of PM, including respiratory disease to cancer and a wide range of global environmental challenges, from acid rain to global warming. Epidemiological studies have consistently shown an association between exposure to PM air pollution during pregnancy and not only the risk of infant mortality and reduced birth weight [4], but also preterm birth (PTB) and stillbirth [5].

Long-term exposure to air pollution has been associated with an increased number of deaths from non-accidental cardiovascular and respiratory disease to lung cancer mortality among older people[3],[6]. However, epidemiological studies and evidence from the last decades have shown the lesser adverse effect of PM exposure on cerebrovascular disease [7].

Considering the World Health Organization assessment, PM2.5 concentration has been linked with premature deaths of almost 800,000 each year, which has the 13th ranking of the cause of mortality in the world [8] . However, additional research and studies prove a more profound relationship than initially expected. The number of data has consistently shown a dose-dependent association between PM exposure and human morbidity in which any decrease of PM from the environment limits the outbreak of these diseases. Simultaneously, more research is required to recognize the effect of PM chemical composition on human health and mortality.

Further studies are strongly shown the problematic consequence of PM pollution on climate change and visibility. Generally, the outcomes of PM on climate change divides into two categories of direct and indirect effects. Direct effects include scattering and absorption of

the sunlight by PM in the atmosphere, whereas indirect effects associate with cloud cover changing by particles serving as cloud condensation nuclei [9]. Besides, decreasing the visibility in the atmosphere due to scattering the light by PM results in a noticeable reduction of the light intensity contrast between a distant object and background sky[8],[9].

Numerous attempts are made to reduce particulate matter pollution from different sources to overcome its harmful impact on humans and the environment. Different organizations provide the regulations for threshold pollutant concentration to protect public health and control air quality. It is also expected that exposure to air pollutants below the threshold concentration provided by the guidelines will not have a dangerous effect on human health.

The particulate matter originated from a different kind of stationary and mobile sources classify either as primary particles emitted directly from a particular emission source (e.g., the smoke of power plants) or secondary particles resulting from the chemical reactions between pollutants in the atmosphere (e.g., sulphur oxides and nitrogen oxides). Particulate matter as a complex mixture of tiny solid particles and liquid droplets is composed of different chemicals. These suspended particles from different sources and of various size vary in composition depending on spatial and temporal scales[11].

1.2. Size of PM:

The International Organization for Standardization (ISO) and the European Committee for Standardization (CEN) have defined several size fractions for airborne particles[11],[12].

The sum of all atmospheric particles is described as the Total Suspended Particles (TSP) or Total Suspended Particulate Matter (TSPM). These parameters often measure by the detecting system without a size-selective inlet.

Inhalable fraction, thoracic fraction, and respirable fraction are other definitions describing the deposition of the particles in the upper (such as mouth or nose) or lower respiratory tract (such as larynx and lungs), respectively. It should also be noted that smaller particles can deeply enter the human body and cause severe morbidity.

For the monitoring purpose, other classes of particulate matter defined by the U.S. Environmental Protection Agency (EPA) (part of a National Ambient Air Quality Standard (NAAQS)) are commonly used [14].

There are four main categories of particulate matter based on their aerodynamic diameter[1], including coarse particles (PM_{10}), fine particles ($PM_{2.5}$), ultrafine particles ($PM_{0.1}$), and nanoparticles.

Usually, PM_x is defined as the total mass of the particles by a diameter of less than or equal to x μm. Figure 1 shows the complete comparison of two size classes PM_{10} and $PM_{2.5}$.

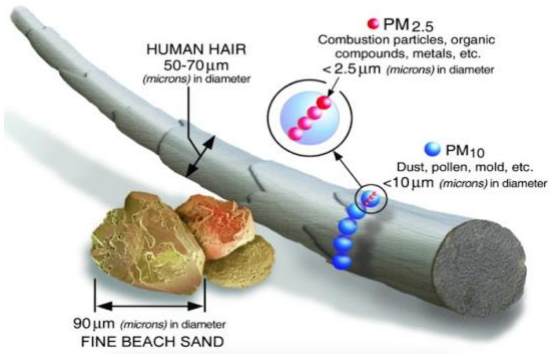

Figure 1. Size comparision of PM10 and PM2.5 [15]

However, the actual definition defined by International Standards Organization is as follows: PM_{10} (respectively $PM_{2.5}$) are *"particles which pass through a size-selective inlet with a 50 % efficiency cut-off at 10µm aerodynamic diameter"* (respectively 2.5µm)[16]. Furthermore, according to the ISO 7708:1995 standard, PM_{10} and $PM_{2.5}$ correspond to the thoracic and the high-risk respirable convention, respectively [12].

As described above, particulate matter can divide by their different aerodynamic equivalent diameter (AED), whereas particles of the same diameter have a similar velocity.

Coarse particles defined as particulates of an aerodynamic diameter ≤ 10 µm mainly include dust, oil, sea salts, pollen, and other parts of plants. They also can be generated during construction, farming, and mining activities. It is worth noting that particles greater than 10 µm are primarily not deposited in the lungs as they are filtered out in the nose and throat [17].

[1] Aerodynamic diameter is defined as the diameter of a 1 g/cm^3 density sphere of the same settling velocity in the air as the measured particle

Fine particulate matters with a diameter of 2.5 μm or smaller can enter into the deep part of the lung. Fine particles mostly produce from various combustion sources such as diesel engines, gasoline engines, wood burning, coal burning for power generation, and non-combustion sources such as ammonium sulfate, ammonium nitrate, and secondary organic aerosols (SOA) [18]. Fine particles also can be derived from industrial processes, such as smelters, cement plants, paper mills, and steel mills.

Ultrafine particles are commonly defined as those less than 0.1μm in diameter. They typically generate from combustion sources, manufacturing of nanomaterials, nucleation processes, or photochemical processes. Ultrafine ambient air can also emit directly from different sources as a primary particle or generate from precursors in the atmosphere as secondary particles [19]. Despite their brief time life, they can overgrow to shape the larger particles (such as PM2.5) through coagulation or condensation. More recently, there has been a general interest in ultrafine particles due to their contribution as a primary source of fine particles. Small ultrafine particles can enter into the lungs and contribute to severe health effects such as lung function decline [20], [21].

It should be mention that another classification suggested by other researchers is considered as nanoparticles with a diameter smaller than 50 nm [22].

Different studies were carried out to extract toxicity scores for particles derived from different PM sources. However, due to the various sizes and chemical components of fine particles, they are not similarly toxic. The results show higher toxicity of combustion than non-combustion aerosols. Among the particulate matter produced from various sources in [18], the highest toxicity score was obtained for exhaust emission from vehicle engine. In this framework, to control and decrease the engine particles level, much research efforts has been spent on developing and designing of the PM detection instruments.

Diesel exhaust particles are probably the most toxic [23] source of ultrafine particles. Although they usually form groups of aggregates with sulphates, metals, and hydrocarbons [24]. The oxidative damage they cause is not only to enzymes and cell membranes but also to DNA, as demonstrated by elevated urinary 8-OHdG levels [25].

In this framework, detection of the soot particulate matter as essential and ubiquitous particulate air pollution is considered during this research.

Figure 2 shows the total overview of four classes of the particulate matter size. PM emission from engines is a combination of fine, ultrafine, and nanoparticles.

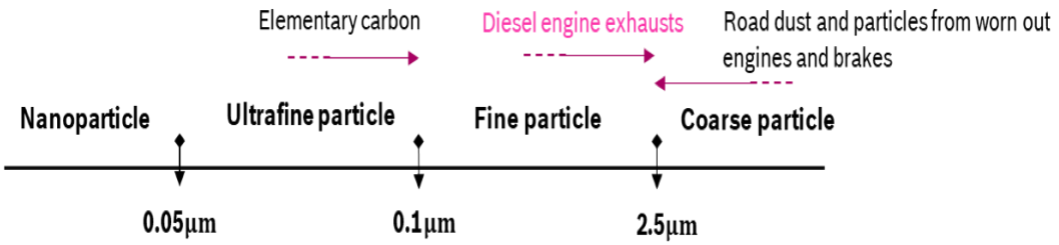

Figure 2. Particulate matter size categories

1.3. Source of Particulate Matter:

It is a critical issue to identify the variety of PM sources contributing to air pollution to take severe actions for reducing air PM pollution associated with human and environmental health. To date, a growing number of evidence on the contribution of various sources to air pollution has been extensively studied. Such studies generally prove that a considerable part of PM is generated from human activities, while natural sources produce a lower portion. Natural source of PM includes volcanoes, wildfires, soil dust, and sea salt whereas anthropogenic sources comprise combustion and industrial processes, traffic, fuel burning, tobacco smoking, candles burning, etc.

Based on European Union (EU) emission report, ambient particulate matter (PM) sources are divided into a total of four categories: Households/small consumers, Energy and industry, Road traffic, and others [26].

Road traffic contributed about 12% of PM pollution in Europe includes different kinds of emissions from various vehicle types. In addition to the primary PM emissions from the exhaust and the emissions of organic and inorganic gaseous PM precursors from the combustion of fuel and lubricant, vehicles emit significant amounts of particles through the wear of brake linings, clutch, and tires [27].

The results of scientific researches carried out in road traffic emissions show that non-exhaust emissions are mainly from the coarse mode of PM (PM2.5-10) while traffic exhaust emissions are mainly to fine PM (diameter < 2.5 mm) [28], [29].

Figure 3 represents the main categories of the pollution traffic sources. The current research focuses on the exhaust emission from passenger cars which is about 16% of the road traffic emissions.

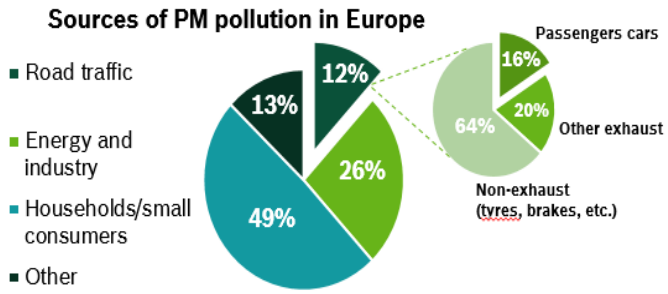

Figure 3. Total overview of the PM sources

In order to overcome the harmful effects of air pollution, it is crucial to pursue a solution to reduce the primary traffic-related PM emissions.

1.4. Composition from diesel engine:

Diesel engines, like other internal combustion engines, transform the chemical energy of fuel into mechanical power. During an ideal combustion process, only carbon dioxide (CO_2) and water vapor (H_2O)is produced by the diesel fuel containing hydrocarbons [30].

However, despite their high combustion efficiency, the small fraction of unburnt fuel and lubricating oil result in many incomplete combustion products [31].

Diesel engine exhaust as a complex mixture consists of solid, condensed (or liquid), and gaseous fractions. The solid fraction mostly comprises elemental carbon with a 10-30 nm diameter that can agglomerate and result in larger soot particles. The solid fraction of the

diesel exhaust engine also includes metal and metal-oxides originating from lubrication and fuel additives, and engine wear [32]. Furthermore, wear on the engine, which mainly consists of iron, can produce nano-sized particles and enrich the carbonaceous soot particles with iron and iron oxides [33]. However, the most common element in the fraction of solid diesel exhaust particles is elementary carbon, which is the primary reason for the black color of the unfiltered diesel emission exhaust.

Figure 4 shows the gaseous exhaust fraction, including non-toxic inorganic gaseous (e.g., nitrogen, water, oxygen) and toxic inorganic gases (e.g., carbon dioxide (CO_2)). Diesel emission exhaust also consists of about 1 percent of pollutant emissions that contribute to severe health problems. The four primary pollutant emissions from diesel engines exhaust are carbon monoxide-CO, hydrocarbons-HC, particulate matter-PM, and nitrogen oxides-NOx.

Most of these pollutants derive from different non-ideal combustion processes, such as incomplete combustion of fuel, reactions between mixture components under high temperature and pressure, combustion of engine lubricating oil and oil additives as well as combustion of non-hydrocarbon components of diesel fuel, such as sulfur compounds and fuel additives [30], [33]. Generally, based on engine type, operation mode, fuel, and lubrication oil type, the composition of the exhaust emission can considerably change [34]–[36].

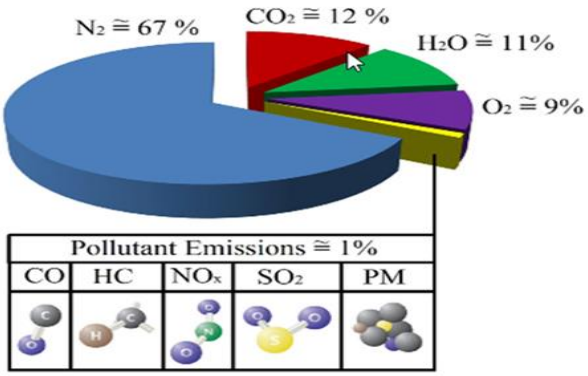

Figure 4.The composition of typical diesel engine exhaust gas[37]

The percentage of PM from diesel emission is still low compared to the total amount of exhaust emission. Figure 4. shows that PM emission contains about less than 1 % of the total

diesel exhaust gasses. However, even this low level of particulate matter can contribute to a hazardous human health effect.

1.5. Particulate matter composition from diesel engine and their structures:

The combustion process of a diesel engine can be defined as unsteady turbulent diffusion combustion [38]. The diesel engine relies upon an auto-ignition of fuel [39], in which injected fuel mixes with intake air inside the chamber. Compressed air inside the chamber generates a high temperature, sufficient for the spontaneous ignition of the diesel fuel [40]. The primary reason for DPM emissions is the presence of a fuel-rich mixture at high temperatures without sufficient oxygen concentration [41], [42] .

Diesel particulate matter (DPM) is a complex mixture of solid and liquid particles suspended in a gas. The chemical composition and physical properties of DPM can be influenced by several factors, such as dilution level, atmospheric processing after emission from the tailpipe, exhaust gas cooling, the working temperature of the engine (e.g., speed/load, injection timing, and strategy), availability of after-treatment equipment (e.g., diesel particulate filter), engine maintenance, photochemical aging, fuel composition (sulfur and ash content) and lubricant used [36], [41], [43].

Diesel exhaust particles resulting from the combustion process include agglomerated solid carbonaceous material, ash, volatile organic, and sulfur components. Liquid phase materials and hydrocarbons absorb on the soot surface and change based on engine operating conditions [44]. As mentioned before, the size, composition, and toxicity level of particulate matter vary depending on many factors. Figure 5 illustrates the nature of diesel particulate matter schematically.

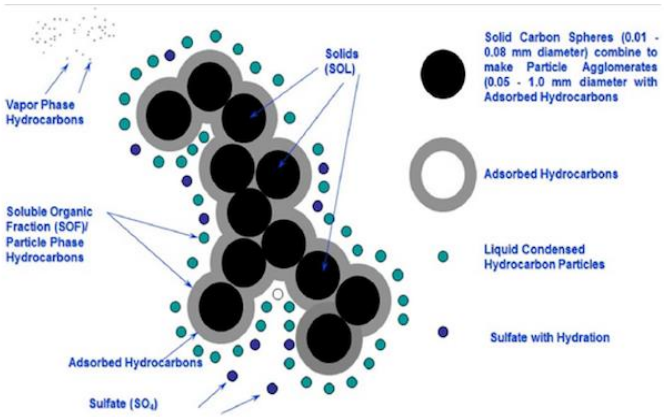

Figure 5.Schematic representation of diesel particulate matter formed during combustion process[41]

Usually, the normal-logarithmic size distribution of the diesel engine particulate matter has three modal structures[44]. Nucleation, Accumulation, and coarse mode are the three main modes of diesel exhaust particulate matter (Figure 6). The peak value of particulate matter number distribution is contained in the nucleation mode, while the maximum value of particulate matter mass distribution is found in the accumulation mode. A small fraction of the particulate matter remains in the third coarse mode, which is not generated during the combustion process [22]. Figure 6 shows a typical size distribution of diesel exhaust particulates matter.

In that figure 6, the expression "normalized" is used to indicate that each of those distributions is divided by the total value of the chosen variable. For instance, if you consider the mass distribution, all the points of the distribution figure are dived by the total mass.

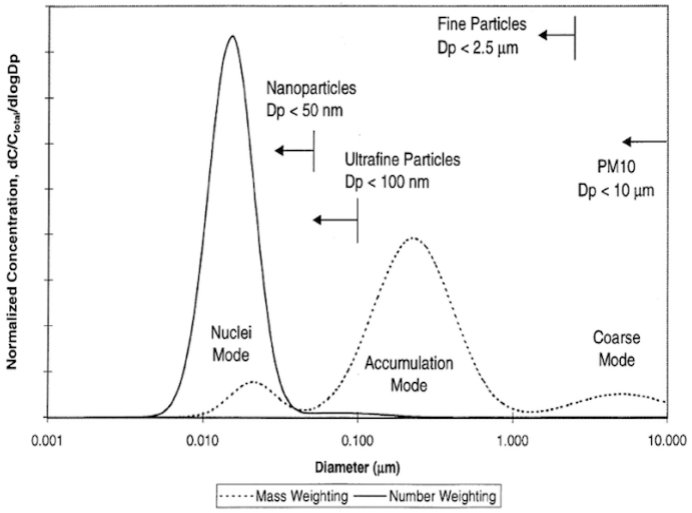

Figure 6.Diesel size distribution [42]

1.6. DPF filter and after treatment system:

Diesel vehicles emit significant particulate mass and numbers in the form of combustion byproducts [45]. To decrease the PM exhaust emissions based on the new regulation, testing different primary solutions such as modification of the engine, fuel, and operating parameters have not fulfilled the requirements. However, the exhaust after treatment (such as catalytic converters and diesel particulate filters (DPFs)) substantially decreases the gaseous and particulate pollutant volumes.

In the last decades, most research activities and studies have focused on developing new technologies for controlling the exhaust emission and reducing the percentage contribution of vehicle emissions to overall ambient PM concentrations.

DPFs are available in multiple configurations, such as ceramic and sintered metal diesel particulate filters. However, the porous ceramic wall-flow is the most commonly used filter. The exhaust emission passes through the walls and collects in the filter. The DPF periodically oxidizes to remove unacceptable pressure-drop across the filter [46].

In brief, DPFs are particularly efficient in controlling most of the soot emissions. Figure 7 shows the size distribution of the particulate matter with and without a particulate filter [47].

The use of the filter guarantees a reduction of two orders of magnitude of PM in the accumulation mode of particulate matter. However, the new nucleation mode downstream of the filter is dominated by volatile materials [47].

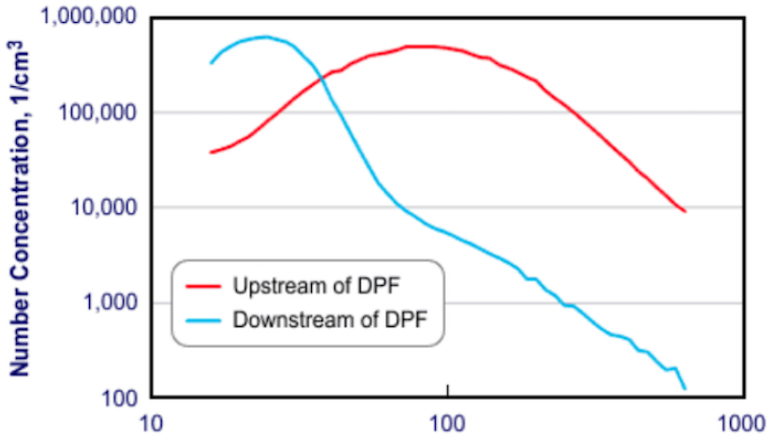

Figure 7.Total Particle Size distribution Upstream and Downstream of Particulate Filter[47]

Although diesel particulate filters are essential for emission control, some DPF failures such as pinhole, crack, fouling, and melt failure, can be observed during the lifetime of the diesel vehicle. In this framework, the filter cannot sufficiently decrease the PM emission and its substrate failures are irreversible [48].

Generally, the DPFs failures result in exhaust emission exceeding and change the PM concentration of vehicle exhaust. Therefore, the regular checking of the exhaust emission to determine any failure of the DPFs is necessary.

Chapter 2 : The total overview of the instruments for detection of the PM from vehicle

2.1. Overview of the methods for particulate emissions detection:

Vehicle exhaust emission has been defined as one of the particulate matter sources [52]. The reduction of PM emission can be obtained by tuning the vehicle engines and exhaust aftertreatment systems. There is a variety of measurement devices based on different principles for the detection of exhaust aerosol. The proposed research aims to choose the most suitable technique for the detection of PM directly after exhaust. In this framework, a general overview of standard techniques and newly designed methods is presented.

However, selection of the best techniques, on the one hand, needs a precise aim of the measurement and definition of the project requirements and, on the other hand, enough information about the characteristics of the methods and devices. The final choice of the sensor is based on monitoring purposes and available budget.

A variety of methods are available to measure particle concentration. Generally, the methods of PM monitoring of the exhaust emission can be divided into two main categories: off-line detection, like the gravimetric analysis, and online detection, e.g., microbalance methods and methods based on mass spectroscopy [53]. However, offline methods use complex and time-consuming techniques and mainly have been used in fixed stations. Besides, the bulky dimension of the devices and their high price are further limitations of the instruments. Online detection systems (e.g., optical methods) rely on the real-time and highly sensitive detection of the particle concentration and has been widely used in industry. Table 2 shows a general overview of the PM measurement methods.

Table 1.General overview of the PM exhaust monitoring device

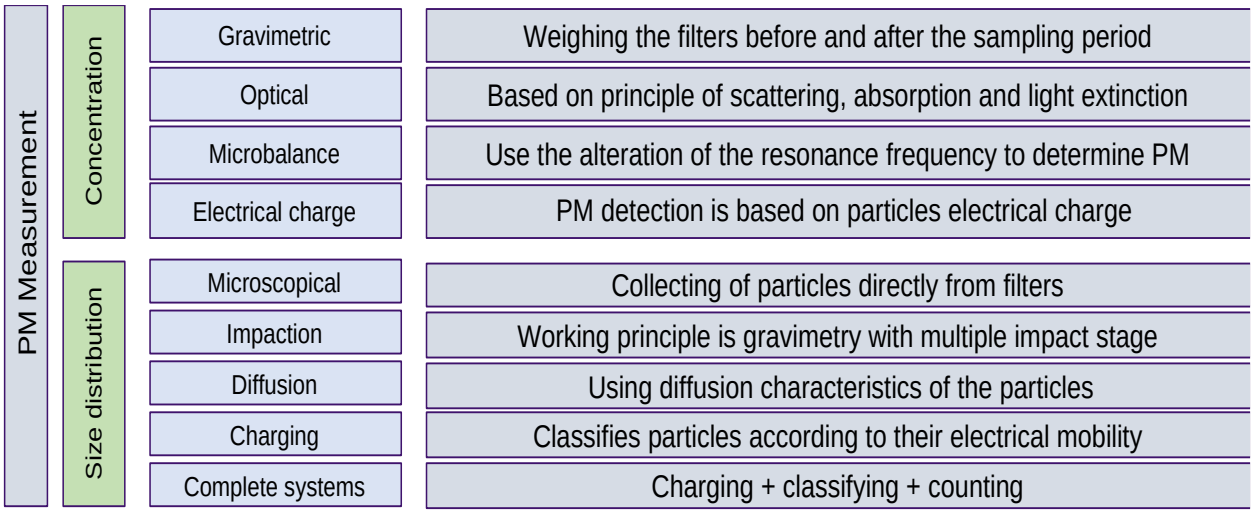

2.1.1. Gravimetric method:

One of the common approaches based on particle deposition for detecting the PM mass concentration is a filter-based gravimetric method. Particle deposits on a filter after dilution in a Constant Volume Sampling (CVS) over a long time, and the total PM mass concentration can be defined by weighting the gravimetric sampler after and before the test. Generally, the filter is able to collect all particle sizes. To select the particular size fraction or remove the large particles, appropriate pre-cyclone is suggested (e.g., cyclone with a cut-off of 10 µm or 25 µm) [54].

The total particle mass concentration can be affected by the filter conditions [53] (e.g., relative humidity or temperature).

Gravimetric filter methods are highly accurate and precise for providing particulate mass concentrations but do not provide temporal information. These high-precision instruments are bulky, stationary and expensive. Therefore, they are not helpful for mobile air quality monitoring. Besides, the detection process is labor-intensive and time-consuming. The system is not sensitive enough for the detection of the modern vehicle emission exhaust. The method needs proper sampling process over a sufficient time to ensure that particle characteristic does not change [55].

2.1.2. Optical methods:

Optical particle sensors based on the interaction of particles with light (e.g., laser or LED) can determine the particulate matter concentration. Optical monitoring instruments based on scattering, absorption, or extinction of light can provide a real-time exhaust measurement. The proposed systems have the advantage of a compact structure for mobile PM monitoring at a reasonable cost. However, there is a limitation of the detection particle size for accurate measurement of the particulate matter.

2.1.3. Light scattering:

The first mathematical model of light scattering was developed in the19th century. Scattering of the light refers to the process where an electromagnetic (EM) wave (e.g., an incident light wave) encounters an obstacle (e.g., a particle), and light photon redirects into a new trajectory. Generally, photon light can deviate from any heterogeneity in the medium that has been illuminated by incident light [55]. Elastic scattering occurs when the wavelength of the scattered light is the same as the incident light. Elastic scattering of electromagnetic radiation by particles can be described by the Mie theory, the Ryleigh theory, and geometry optics [56].

A size parameter of the particles can be defined by the following formula [56] :

$$x = \frac{2\pi r}{\lambda} \tag{1}$$

where r is the particle length (radius), λ is the wavelength of the incidence light and x is the size parameter.

Mie theory is usually valid when particles' size is comparable to the wavelength of light, i.e., $x = 1$. Generally, when the particle size is much smaller than the light wavelength, i.e., $x \ll 1$, Mie theory converges to Rayleigh scattering. For $x \gg 1$, Mie scattering theory gradually converts to geometric optics with the increase of particle size. There is no size limitation for

Mie theory, and it can be applied to different scattering systems. However, because of the Mie theory 's complicity, it is likely to use Ryleigh theory for small scales particles.

The light scattering-based sensors can detect the scattered light intensity of the single particle (e.g., optical particle counters and condensation particle counter) or a group of particles in the observation volume (e.g., scattering-based photometer) .

The main idea to adapt smoke alarm system to PM monitoring sensor was suggested in 1994 within the context of planned work in Guatemala as part of the research organized by the World Health Organization [57]. The aerosol particles enter the optical sensor zone by the use of a pump, where the intensity of the scattered light detect at one or more angles [7,6]. However, the instrument does not have enough accuracy for the detection of the small particles.

Optical particle counters (OPCs) are among the most commonly used light scattering-based instruments. The first light scattering-based counter was introduced in 1940 [59]. Up to now, several improvements in terms of performance, dimension, and accuracy have been achieved.

The functional operation of an OPC relies on the light scattering methods, e.g., Mie theory and Ryleigh theory. The inlet nozzle directs the particles to cross a laser beam, and each particle scatters the light in all directions. The photodetector receives the scattered light from the particles and generates a current pulse proportional to the particulate matter size. Since the detected scattering light amount is a function of particle size and composition, it is necessary to perform a calibration process, that can be assessed by using monodisperse particles [60].

One of the standard instruments for detecting number concentration is the condensation particle counter (CPC) that uses light scattering to count the particles after magnifying their size [53]. The number concentration can easily determine by measuring the pulses from each particle and the sampling flow rate. The European regulation needs a 50% counting efficiency at 23 nm. However, the cut-off should be defined by selecting an acceptable saturation ratio [61].

Generally, the particles growth occur while aerosols pass through the saturated vapor (e.g., n-butanol as working fluid). The temperature of the saturated particle decrease in a condenser before exposure to the laser beam. Since selecting an appropriate saturation ratio is essential, the saturator and condenser temperature remains in the limited range. Therefore, there is always a challenge for using the device in outdoor temperature [61].

2.1.4. Light absorption:

Black carbon (BC) is the most robust visible solar radiative absorber contributing to climate change in the atmosphere [62]. There are different optical sensors based on light absorption for detection of the PM mass concentration.

In a spotmeter, the filter smoke meter (FSN) and the particle concentration can be measured by filtering exhaust through a paper filter and recording the ratio between the light reflected by this exposed spot and an unexposed spot [53]. The sensor is among the robust measurement instrument which can use in the engine test cells. The reflectometer can also determine the mass concentration of the raw exhaust emission [63].

In an aethalometer [64], the sampled particulate matter collect through the filter and create a patch of increasing density. The increasing of the attenuation of the laser beam over time is proportional to the PM concentration on the filter. Various parameter such as the filter structure, the distribution of the particulate mass on the filter and angular distribution of scattered light can affect the measurement results.

Photoacoustic Soot Sensor (PASS) is based on photoacoustic measurement techniques [65]. The sampled airflow exposes to the modulated laser beam. The particles periodically absorb the light energy and heat up, which creates the sound waves [66]. The sound wave frequency can be detected by the use of the microphone. The recorded sound signals are linearly proportional to particles concentration in the measuring volume [67].

In Laser induced Incandescence (LII), particles heat to the high temperature with a high-power, pulsed, or continuous-wave (CW) laser to emit measurable quasi blackbody radiation. The radiation records with different detection techniques (e.g., time-resolved , time-integrated detection methods). In addition to the refractive index, the signal is affected by the laser intensity, incandescence collection optics, and sensitivity of the detector [68].

2.1.5. Light extinction:

Light extinction measurement is provided by the sum of the absorption and the scattering of the light. Extinction detection are performed by opacity meters and cavity-ring-down devices but only the former have been used in exhaust aerosol studies [53].

Opacity meters are widely used for monitoring the PM emission from diesel engine by detecting the light transmitted through a given light path. However, the opacity can vary with particle size, the wavelength of the light source and the shape of the particles.

In fact, the opacity is just a relative indication of the real particle mass concentration. For example variation in particle size [69] or PM physical condition can affect the calibration between opacity and mass concentration [70]. In addition, as progress is made in reducing the particulate emissions, the sensitivity of conventional opacity meters becomes inadequate [71]. Opacity meters are still an easy and efficient soot determination method for the engines, however, their detection limit for DPF-equipped engines is very high.

2.1.6. Microbalance methods:

In microbalance methods, the particles collect on an oscillating element or a piezoelectric resonator [72]. The PM mass concentration can be determined by changing the natural frequency of the oscillator through the collected particle.

Microbalance methods are not useful for detecting vehicle emissions due to their problems with humidity, temperature, and overloading. Besides, the device is expensive, and its dimension is quite extensive. It is also necessary to clean the sensor frequently.

The tapered element oscillating microbalance (TEOM) and the quartz crystal microbalance (QCM) are two online methods for determination of the mass concentration based on alteration of the resonance frequency.

Both techniques have a good time resolution and enough sensitivity. However, for the TEOM method, uptake of water and other volatile material may result in artifacts[73]. The main problem of quartz crystal microbalance [74] is that the total mass loading can affect the instrument performance.

Furthermore, some developments of miniaturized and portable devices based on high-frequency acoustic techniques are reported [75]. Generally, based on the propagation of the acoustic wave neither through the piezoelectric crystal, e.g., film bulk acoustic resonators (FBARs) [76] or parallel to the surface of piezoelectric material, e.g., Surface acoustic wave (SAW) [77], two main categories of the acoustic devices can be considered. The PM mass deposition on the piezoelectric surface (due to the thermophoresis effect) and changing the resonance frequency can result in high accuracy measurement of the accumulated mass. However, due to the need for piezoelectric substrate, the system manufacturing process, and fabricating electronic components, the sensor is complex [75]. Because of the high cost associated with the manufacturing process, these devices are not commonly used in air quality monitoring. Besides, one of the main concerns regarding the use of the acoustic sensors after tailpipe can be related to changing the resonance frequency of the piezoelectric crystal due to tailpipe vibrations.

2.1.7. Electrical charge based methods:

The simple designed and sensitive PM sensor based on the particle's electrical charge for detection of the PM concentration has been proposed. Photoelectric aerosol sensors (PAS) based on photoemission charging are not used in the automotive field as they are highly dependent on the composition surface of illuminated particles [53].

Diffusion Chargers (DC) are mainly used as compact, robust, and lightweight sensors for particle number concentration measurement. Generally, DC consists of the particle charging and subsequent detection of the current. Firstly, a corona discharge generates unipolar ions which attach to the particle surface. In the second step, the electrical current is measured by the use of an electrometer. This current is proportional to the particle active surface and does not directly represent the particle number concentration. Therefore, the number concentration can be achieved through additional calculation. The accuracy of the method can be estimated at 25% [53].

The first prototype to adapt diffusion chargers for detection of the number concentration of raw engine exhaust was successfully designed [78]. However, continuous mountainous and

cleaning due to exhaust emission temperature, the variation of flow rate, and direct exposure to exhaust emission were necessary.

The alternative version by the use of an integral ejector pump was suggested [79]. The sensor provides a fixed flow rate and protects the corona from exposure to pollution. Recently, Rüggeberg [80] et al. was introduced a modified version of the sensor. The system can operate at more than 150 ℃ and does not need dilution. However, the sensor has a high weight (about 10 kg) and bulky size.

2.2. Size distribution methods:

2.2.1. Microscopy:

Microscopy methods rely on collecting the particle in the filter and analyzing them [81] to provide the size distribution of the particles. In addition to their size, electronic microscopy examines the morphology of the particles. Scanning electron microscope (SEM) and transmission electron microscope (TEM) images can detect size distributions manually or more commonly by automated digital image analysis. Image analysis (e.g., transmission electron microscopy) can also offer a wide range of information regarding the soot aggregates (e.g., radius, size, dimension) [82]. The images usually represent a two-dimensional particle projection. However, the projected area of diesel agglomerates is closely related to their mobility diameter [83].

The main problem of the microscopy method is that; it takes time to analyze a number of particles that is statistically adequate. The electron microscopy method is also useful for determining the effect of fuel composition or engine operation on soot morphology [84].

2.2.1. Impactor:

Impactors are a valuable device for the detection of mass-weighted size distribution. They work based on gravimetry, with multiple impact stages. The most widely used devices are cascade impactors that operate based on particles' inertial classification [85].

The aerosol sample goes through a series of stages. In each stage, the aerosol sample passes through an array of nozzles above a solid substrate. Particles above the cutoff diameter

collect by impaction; however, small particles follow the gas flow that surrounds the collection plate and deposit in the following stages [85]. This method continues until smaller particles collect in the final filter. Having a narrow nozzle as well as high-velocity airflow have the advantage of collecting the smaller particles.

Due to their size limitations, cascade impactors are primarily used in atmospheric research and are not effective in vehicle research. Impactors are affected by bounces, where particles do not adhere to the impactor surface due to their sampling flow rate. They are also susceptible to clogging, where contaminants bind to walls and nozzles.

The Electrical Low Pressure Impactor (ELPI) is another relatively new impactor designed to detect aerosol particles' size distribution in the range of 0.03 to 10 μm diameter. The device work on the electrically charging of the particles [86].

2.2.3. Diffusion battery:

Diffusion Batteries have been developed to detect the diffusion coefficients of the particles [35] for several decades. Diffusion batteries separate particles by their mobility and determine the size distribution from the particle diffusion characteristics.

The electrical diffusion battery (EDB) is a new method in which particles charge with a corona charger before going through the diffusion battery [87]. The screen-type diffusion battery stages are electrically insulated, and each of them connects to a current amplifier to determine the particle size distribution [88]. The portable device based on this method is quite simple and robust. The downside is the sensitivity of the diffusion screens to being dirty with the accumulated particles, which specifically affects size and quantification.

EDB collection efficiency depends on geometric properties of the tube, the flow rate, and particle size, expressed in terms of equivalent diameter in volume [31].

2.2.4. Mobility analyzer:

The first mobility analyzer, Electrical Aerosol Analyzer (EAA), for detection of the ultrafine aerosol particles was successfully introduced in the 1960s, and with time the EAA has replaced by the more advanced Differential Mobility Analyzer (DMA)[89].

Aerosol particles electrically charge in a unipolar corona charger. Particle below specific electric mobility passes through an electric mobility analyzer and detect by the use of the electrometer. There is a significant number of DMAs in the literature [90]. In order to impart a well-defined Fuchs charge distribution, DMAs use bipolar diffusion charging [3]. Then particles after passing the electrostatic classifier can be measured by a CPC or an electrometer. The applied voltage can be ramped to a scan over a particle diameter range in few minutes using Scanning Mobility Particle Sizer (SMPS) [3]. It is also an accurate device for to determine the high-resolution size distributions from exhaust emission.

2.2.5. Differential mobility spectrometers:

The most widely recognized spectrometers based on particle mobility are the Differential Mobility Spectrometers (DMS) [91], the Fast Mobility Particle Sizer (FMPS), and Engine Exhaust Particle Sizer (EEPS) [92]. They include a particle charger, a classifier, and a series of detectors.

A corona diffusion charger provides a unipolar charge distribution on the particles. They pass along the periphery of the central rod of a classifier connected to a series of sensitive electrometers. The provided current convert to number distribution of the particle over the electrical mobility range of the instrument [93]. Scanning Mobility Particle Sizer (SMPS) and Twin Differential Mobility Particle Sizer (TDMPS) are also used to detect particle mobility.

The SMPS has higher sensitivity compared to mobility spectrometers. However, spectrometers are sufficiently adaptive to calculate the size distributions in the automotive field [93] .

2.2.6. Electrical Low Pressure Impactor (ELPI):

The size distribution of particles based on aerodynamic diameter can be calculated by the use of electrical low-pressure impactor [86]. The aerosols are charged using a unipolar corona charger. Then they enter the cascade impactor composed of electrically isolated

collection stages. The electrometer detects the electrical current produced by particles in real-time. In EPLI, particles categorize based on their aerodynamic diameter. The particle concentration depends on the calibration of the corona discharge, impactor collection efficiency, and measured current [3]. The use of the ELPI for low emission vehicles is not recommended due to the reduction of mass detection accuracy by the use of filter [94].

Recently, Dekati Ltd. has released an updated version of this instrument [95]. This ELPI Plus impactor has 14 stages enabling measurement a size range of 6 nm to 10 m with a 10 Hz sampling rate.

Other instruments such as Centrifugal Particle Mass Analyzer (CPMA)[96] are not mainly used for emission exhaust testing. Because of their limitations and little applications to emission testing, they are not discussed in this section.

2.3. Periodic technical check of the emission from diesel vehicle

A number of limitations from diesel vehicle for type approval checking were established by the European Union. In Europe, a large percentage of diesel-powered cars are fitted with efficient particle filters. It was assumed that on-board diagnostic (OBD) systems could determine the performance of the filter and recognize the high polluters vehicle. However, data from on-board diagnostics systems are not always reliable to recognize the defected filters. The obtained data from OBD can be illegally manipulated after removing the aftertreatment systems by the end-users [97].

Currently, the periodic emission check for diesel vehicles is based on smoke opacity, which has a low correlation with PM/PN emission. Furthermore, available opacimeters have an accuracy that is not suitable to measure low smoke emission levels [97]. As mention in 2.2.1, CPC is a standard instrument for the detection of number concentration measurements.

The TSI Nanoparticle Emission Tester (NPET) Model 3795 [98] is designed to detect the number concentration of the combustion engine (e.g., diesel engine). The sensor features a dilution system, a catalytic stripper for removing the volatile particles, and a CPC. Besides, the system fulfills the requirement of the Swiss regulation SR941.242. The SENSORS

company introduced another condensation particle number (CPN) [99], which follows the EU RDE PN-PEMS measurement requirements.

The main concern regarding both systems is their bulky dimensions, high weight, and their cost. For this reason, the condensation particle counter is not appropriate for applications far from the laboratory environment.

Besides CPCs, instruments based on diffusion charging (DC sensors) can detect the PM concentration. However, there are some limitations to the successful use of DC sensors. Firstly, the sensor response considerably depends on the size of the particle. In this case, different fuel blends and engine loads affect the system accuracy. Secondly, the sensor cannot follow very precise counting efficiency requirements.

Thirdly, the system is not able to directly detect the number concentration. Therefore, additional information of the particle size distribution for converting the measured current to particle number concentration is required. This process needs signal manipulation, and till now there is no calibration standard to ensure accuracy of detection [100].

In this framework, DC sensors are not anymore a candidate for the detection of DPF performance and particle concentration of the vehicle exhaust and more work is needed to find an adequate solution.

Therefore, designing a low weight and cheap equipment to detect emissions after tailpipe would enable a fast and affordable analysis of DPF filters performance and faults. This work proposes the theoretical design of a new cheap and simple detection system to measure the PM concentration after tailpipe and monitor the DPF performance. Therefore, the choice of a suitable particle sensor aims at obtaining a compact detection system appropriate for real-time measurements of PM concentration.

2.4. Selection of the best method for detection of PM concentration after exhaust

In order to design a layout for PM detection after exhaust, it is necessary to select a suitable method for measuring the particle concentration. However, to determine the DPF performance, both mass and number concentration can be considered.

Chapter 2 describes an overview of possible methods for detecting particulate matter from vehicle exhaust. For selection of the best method, it is necessary to compare the sensors based on the requirement of the project.

The essential features to choose the appropriate method for detecting the DPF performance and faults are listed below. These five characteristics for different PM detection methods are compared in tables 3.

1- Real-time detection: It is necessary that the sensor provides real-time information with no delay in detecting of particulate matter concentration.
2- Compact structure: Since the effects of long-term and short-term exposure to PM are considered hazardous, a periodical check of the exhaust emission is necessary. The final aim of the project is to have a compact device that can directly use in the back of the vehicle for regular test of the PM emissions.
3- Sensitivity: The method should be sensitive enough for the determination of PM after vehicle exhaust.
4- Easy to use: The sensor does not need frequent cleaning and maintenance (such as replacement of filter, cleaning the deposition, etc.)
5- The cost of the sensor: Since the goal of the project is to develop the commercial sensor, the overall expense of the system is one of the most significant features in the design of the final layout. It is expected that the accuracy of the simple, compact instrument is lower than that of expensive stationary devices. However, cheap PM detection equipment helps developing countries to build inexpensive measurement sensors for exhaust PM monitoring purposes.

Table 2. Methods for PM measurement_ First Selection

Principle	Real time	Compact structure	Sensitivity	Maintenance (e.g. Frequent cleaning, filter replacement)	Cost
Gravimetric	🔴	🔴	🟢	🔴	🔴
Optical	🟢	🟢	🟢	🟡	🟢
Microbalance	🟢	🔴	🔴	🔴	🟢
Electrical charge	🟢	🔴	🟢	🟡	🔴
Microscopical	🔴	🔴	🟢	🔴	🔴
Impaction	🔴	🔴	🟢	🔴	🟢
Diffusion	🟢	🔴	🟡	🔴	🟢
Charging	🔴	🔴	🔴	🟢	🔴
Complete systems (charging+ classifying+ counting)	🟢	🟡	🔴	🟢	🔴

Red : Negative, Green : Positive , Yellow: Medium

In the first selection (Table 3), the optical methods seem promising to fulfill the requirement of the project. However, the working principle of optical sensors is based on three different method of scattering, absorption and extinction. Table 4 shows the summery of the optical based methods for detection of the PM.

Table 3. Total overview of the optical methods

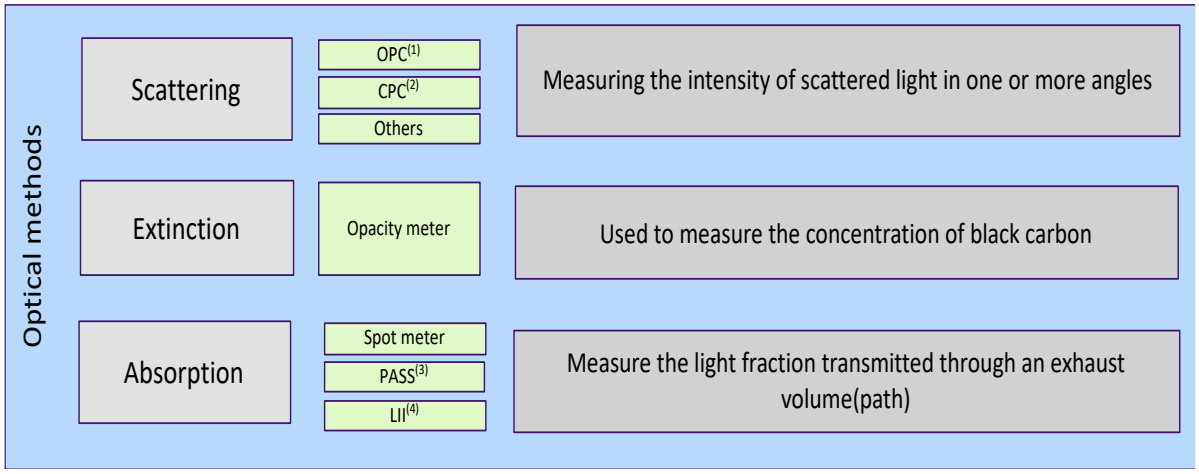

(1)Optical particle counter , (2)Condensation particle counter , (3)Photoacoustic Soot Sensor, (4)Laser Induced Incandescence

In the second selection, methods based on the scattering principle fit the requirement list of the work. Accuracy refers to instrument bias and repeatability and is estimated based on its calibration standards. The accuracy of the scattering methods is about 30% which is acceptable according to the requirement list.

Table 4. Scattering methods for PM measurements - Second selection

Principle	Dilution required	Complexity	Accuracy (%)	Detection limit	Necessitate calibration	Size range (nm)
Scattering	No	Low	30	$10\frac{\mu g}{m^3}$	No	>50
Extinction	No	High	15	$5\frac{\mu g}{m^3}$	No	>50
Absorption	Some instruments need*	Low	20	0.1% opacity	Yes	>10

*) some instrument need dilution such as PASS, and some doesn't need such as LII

Among the scattering-based sensor, considering the size, cost, and simplicity, the optical particle counter can be a good option for monitoring the PM after exhaust. In the next chapter, to find the best solution, different scattering-based sensors for air quality monitoring available in the market and under research will be considered.

Chapter 3: The overview of the scattering based device (Optical particle counter) for detection of the PM

3.1. Selection of the best instrument for detection of PM after exhaust

In chapter 2, different available methods for the detection of PM after exhaust was discussed. Based on the requirement of the project, the optical method based on scattering was selected. Among scattering-based sensors, optical particle counters (OPCs) as small, low-weight, and low-cost sensors can be the best choice for PM detection directly after diesel tailpipe. The proposed sensors are widely used in outdoor and indoor air quality monitoring. In this chapter, the general structure of the commercial optical particle counters is described and the newly designed OPC from recent papers is compared.

3.2 . Optical particle counters and air quality monitoring

During the last decades, various air quality monitoring techniques such as gravimetric, electrostatic, and thermal methods were developed. However, they are mainly high cost and used in fixed stations. Since the concentration of PM varied at the local scale, and fixed monitoring stations are not enough in the urban sites, low cost and mobile PM monitoring has attracted much attention. Among a great variety of techniques, light scattering methods give the opportunity to build portable and compact devices (e.g., Optical particle counters (OPCs)) suitable for real-time detection of PM concentration. However, it is compulsory to conduct more research on different sensor structures to improve the performance of the low-cost OPC.

3.3. General structures of the optical particle counters

There is an increasing interest in the application of low-cost OPCs for PM air monitoring. The significant advantages of these low-cost devices are their small size and low power consumption.

The operation principle of the optical particle counter is usually described by Mie scattering theory or Rayleigh scattering theory. The airborne particles are illuminated by the collimated

light beam e.g., laser or LED light and scattered in all the directions. The proportion of the scattered light using lens or mirror is focused on the optical photodetector and generated a signal peak proportion to the particle size. As the intensity of the scattered light is weak, it is necessary to design the light trap at the far end of the light beam to suppress the stray light.

3.4. New designed optical particle counters

There are various low-cost scattering optical particle counters on the market, which usually have similar structures. Recently, novel optical particle counters have been proposed by researchers to improve the accuracy of the instruments and decrease the device dimensions. This section presents an overview of the most recent advances in mobile, low-cost OPCs.

3.4.1. Mobile Phone- Based OPC:

A light scattering optical sensor based on a smartphone for monitoring of PM has been recently developed [101]. The proposed system is based on the combination of a cell phone with a low-cost optical device. The LED flash of the phone with a mirror illuminates the particle, then a series of photographs are captured by the camera (as the photodetector). The final concentration of PM can be estimated by analyzing the captured images and considering the scattered light intensity [102].

Moreover, by applying a single large magnify lens together with the 2-D sensor camera, it is possible to obtain the virtual image of the dust particles in observation volume [103].

This provides additional information on the light scatter traces of the individual particles. Fig.8 shows the total design of the light scattering sensor using a smartphone. It should be noted that the proposed sensor can be easily mounted and detached when unused.

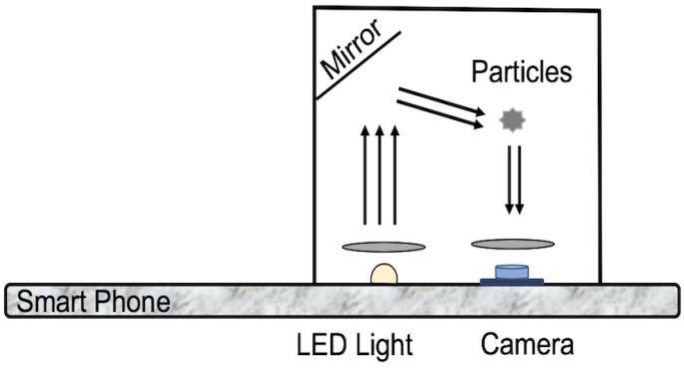

Figure 8. OPC design depending on LED and camera of the smart phone

3.4.2. CPC-Based OPC:

Recently, a novel particle sensor based on complicated parabolic collector (CPC), which collects a wide angle of scattered light from particles, has been proposed. The cylindrical sensor (11 mm × 25 mm) offers high sensitivity in the detection of the sub-micro particles without using a filter. The laser diode illuminates particles, and a photodiode detects the proportion of the scattered light collected by CPC [104].

Through numerical analysis, monitoring of particles with an aerodynamic diameter of less than 1.0 μm requires an acceptance angle of CPC of 20° . Furthermore, compared to other systems based on 90° scattering and back scattering, the proposed sensor can obtain a lower resolution of 7.9 $\mu g/m^3$. Since the sensor resolution is lower in comparison with the level of 24-hour PM2.5 in WHO standard (limit to 25 $\mu g/m^3$) [105], it can be used for air quality monitoring. Fig. 9 shows the schematic view of the sensor.

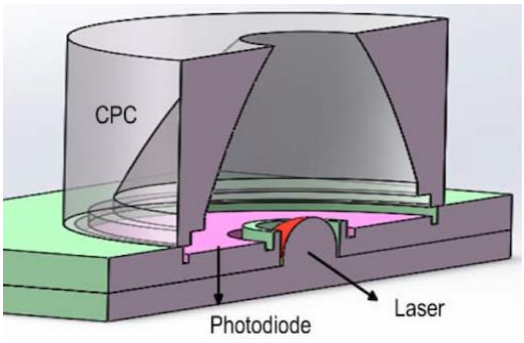

Figure 9. General schematic of the CPC-based device

3.4.3. Silicon- Based OPC:

Another interesting miniaturized PM sensor, still based on light scattering, is formed by two silicon submounts attached using adhesive bonding [106]. Both of silicon wafers are made separately using a microfabrication process. In the bottom wafer, two pairs of laser diodes as light sources and photodiodes as detectors are inserted into cavities, whereas the top submount just includes the airflow channels. In the sensing chamber, the collimating channel can be enhanced to eliminate the laser direct incident light to the photodiode and concentrate on the scattered light.

Besides, a virtual impactor (VI) is integrated into the top wafer and after the air inlet as a particle selector. It is assumed that the airflow rate is very low if using VI in the top submount, which contributes to the sensor low power consumption [107]. The airflow containing the particles, flows through the inlet and enters the VI by a jet. In this framework, sampling particles go through the sensing chamber, and the large particles go out from the outlet.

Fig.10 shows a miniaturized sensor with a size of 15mm × 10 mm × 1mm.

Compared with the previous version [108], the contribution of multiple factors leads to a better performance in terms of the system mass detection accuracy. As the particles behavior of various range size, describe by different light scattering theories, the selection of the fine particles by the VI filter can provide more accurate mass concentration. Besides, the improvement in the packaging reduced the detection noise of the system. As a consequence, experimental results indicated a limit detection value of the sensor of 2.55μg/m^3 .

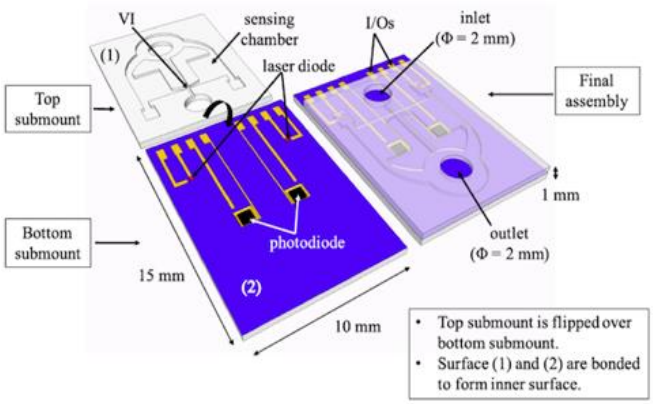

Figure 10. Final Layout of the silicon microfabrication based OPC[108]

3.4.4. Fresnel Ring Lens - Based OPC:

Miniaturized optical particle sensor capable of collecting the scattered light at two solid angle section by Fresnel lenses, can monitor the mass concentration of the particles. The system configuration includes two subsystems; the first part uses inertial filtering with an impactor filter (IF). The filter is connected to the inlet of the optical particle sensor to separate the desired particles.

The second part, which determines the size distribution of the particles, is based on the light scattering. The airflow passes through the inlet nozzle, illuminated by the laser beam, and the particle size can be determined by detecting the intensity of the collected scattered light using two avalanche photodiodes.

In order to collect the scattered light, the system uses the Fresnel lenses instead of spherical lenses that are typically used in optical particle sensors. Fig. 11 represents the overall layout of the sensor system [109].

In the overall structure of the optical particle system, three Fresnel ring lenses (with large numerical aperture) place in the forward scattering direction. The first frontal Fresnel lens, at the centre, spans around the laser beam trap, collects and collimates the scattered laser light. The other two Fresnel lenses (behind the main lens as off-centre ring lenses) image the light into two avalanche photodiodes (APD) with separate angles [110]. Finally, particle mass concentration is calculated by multiplying the density and determined volume of particles.

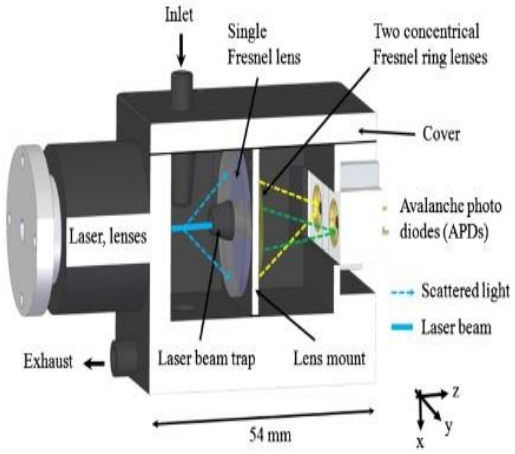

Figure 11. Scattering system for OPC detection using Fresnel lenses

3.4.5. Drilled Lens - Based OPC:

There is a significant need to increase the sensitivity of the OPC by detecting the forward scattered light from the small particles. The new plastic lens with a hole drilled is proposed to optimize the collection of the forward scattered light and detect the small particles. In fact, the laser beam can be separated from the scattered light by means of the drilled lens (Fig. 12).

The particle entering from the air jet (upstream of the lens back focal plane) is illuminated by the laser beam and scatters the light mostly in the forward direction. The laser beam passes through the small hole drilled (in the off- axis lens) to a light trap. Then the scattered light can be collected on the opposite side of the drilled hole, (off-axis from the lens centre) and detected by the optical detector. Finally, detecting the amplitude of the scattered light by an optical detector ensures that the particle size is determined by a defined refractive index [111].

The proposed device is usually cost-effective and not complicated, but the small numerical aperture of the aspheric lens and the diameter of the hole drilled in the lens can be a limitation for the angular range of the light collection [111].

It is worth to notice that the light scattered OPC device is appropriate for balloon-borne and ground-based PM monitoring.

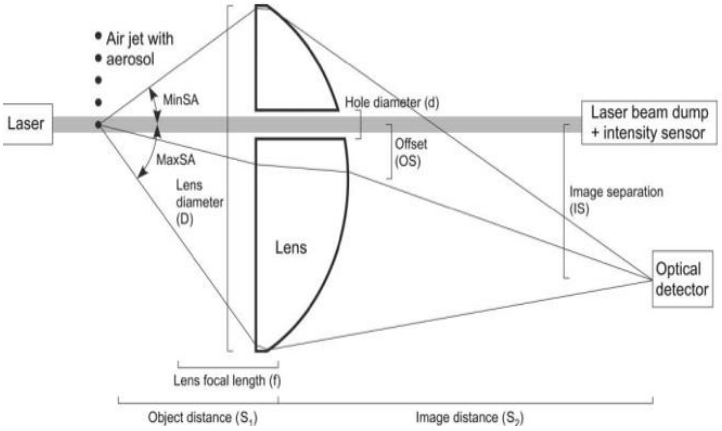

Figure 12. Structure of the sensing chamber using drilled lens

3.4.6. Comparison of Recent OPC Structures:

Table 1 summarizes the characteristics of the considered technological solutions. Each type of sensor is more appropriate for a specific PM size range, depending on the different structure of the sensor. The Table shows that the system based on the Fresnel lens enables the smaller detection size of 125 μm. Although the overall system structure is quite small, using two sensitive avalanche photodiodes and Fresnel lenses can increase the sensor cost.

Among them, miniaturized camera-based OPC depends on the phone model. The major drawback of this sensor is that using the smartphone LED flash as a light source restricts the measurable particle size. The advantage of the proposed sensor is its ultra-lowcost.

Silicon-based OPC has also a miniaturized scale and low power usage and can be used in both smartphone and smart watches. However, due to use of specific components in each system (such as detectors, lens, etc..), the total cost of the device should be higher than commercial OPC in the market.

Table 5.Comparision of newly designed OPC

Kind of sensor	CPC-based OPC	Silicon-based OPC	Drilled lens based OPC	Fresnel ring lens-based OPC	Camera - based OPC
Working principle	Light scattering	Light scattering	Light scattering	Light scattering	Light scattering + signal processing algorithm
Detected PM size ranges	PM_1	$PM_{2.5}$	$PM_{2.5}$ (PM above 140nm)	$PM_{2.5}$ (PM above 125 nm)	$PM_{10-2.5}$
Minimum Resolution	7.9 $\mu g/m^3$	2.55 $\mu g/m^3$	-	-	-
Detection system	Mass concentration	Mass concentration	Mass concentration	Size detection / Mass concentration	Size detection /Mass concentration
Light detection	Laser diode (635nm)	Laser diode (650nm)	Laser diode (405nm)	Laser diode (450 nm)	Smartphone flash LED
Detector Photomultiplier	Five red-enhanced Si photodiode	Silicon PIN Photodiode	Photomultiplier	Two avalanche photodiodes	Smartphone camera
External Lens	CPC-20°C Acceptance angle	Collimating channel	Aspheric lens with hole	Fresnel ring lenses	Large magnification lens
Reference system	Dust track DRX TSI18533	OPC 1.109 GRIMM	Single particle soot photometer	Grimm SMPS+C5.403	SMPS/ TSI APS
Dimension	Miniaturized (11mm*25mm)	Miniaturized (15mm*10mm*1mm)	Small (length:260mm)	Miniaturized (Measurement chamber:54mm)	Miniaturized (Depend on Phone model)

Chapter 4 :Detection of particulate matter using the new developed camera-based optical sensors

4.1. Drawback of the optical systems based on scattering and selection of the best instrument for monitoring PM

Between the detection methods of PM, scattering based optical sensor seems a promising device to use after exhaust pf the vehicle. Optical systems based on the light scattering method enable real-time detection of particle concentration using optical particle counters (OPCs).

However, the major drawback of the light scattering method is the increasing probability of coincidence at high densities which affects the accuracy of the detection system. To overcome the error, using an appropriate dilution system or changing the OPC structure was suggested.

In order to find a simple and low-cost detection system, it is necessary to review and compare the newly designed, low-weight, compact optical devices for air quality monitor. Then we are able to decide whether the proposed sensors are suitable to use in the tailpipe or not.

Currently, the researchers are introducing newly designed camera-based optical sensors using different software and hardware. This paper presents an overview of the most recent advances in proposed sensors.

4.2. Newly designed camera-based optical particle sensor

Hazardous effects of particulate matter on human health and the environment have stimulated growing demands for developing low-cost, portable, and reliable PM monitoring sensors.

However, the mobile PM detection sensors are a much less known area compared to significantly numerous reports of the classic air monitoring techniques.

Nowadays, the newly designed camera-based sensors have been developed by researchers to provide a portable and accurate detection system.

4.2.1. Filter-based particle sensor

Another impressive low-cost sensor based on a glass-fiber filter and camera can be used for PM monitoring in the urban environment [112], [113]. The particulate matter transported by the airflow goes into the inlet sampling and passes through the filter with the help of a small low power pump (Fig. 13).

Inside the chamber, the filter surface illuminates by a set of multi-wavelength LEDs light. The front camera periodically takes photos to detect the captured particles on the filter.

Finally, image processing software provides the size distribution of the particulate matter from recorded images[114]. The image processing software uses the OpenCV library and performs four processing phases to analysis the captured image.

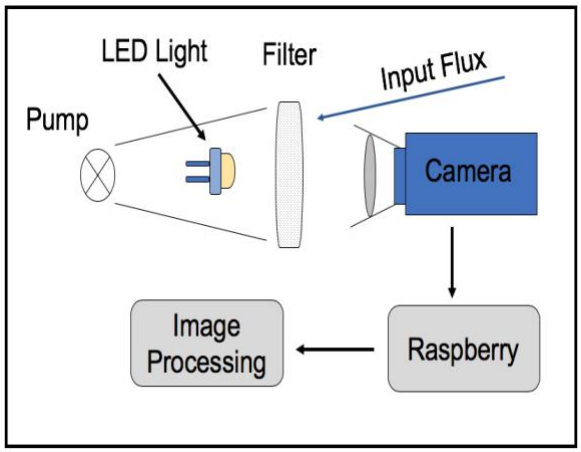

Figure 13. Block diagram of the filter based particulate matter sensor.

4.2.2. Dust deposition camera particle counter

A novel approach based on CMOS image sensors using image processing techniques, classification algorithms ,and pattern recognition is proposed [115], [116].

In the proposed sensor, the dust directly deposits on the CMOS image sensor (without any lens). The sensor was placed at 45° angle towards the ground to restrict the overlapping due

to particle accumulation[115]. An LED lamp light illuminates the sensor surface to obtain high-contrast photos in different environmental conditions.

The control software allows taking a picture periodically and saves it as an uncompressed JPEG. Image processing algorithms enhance the captured images characteristics (e.g., contrast). Consequently, the particle size and shape can be obtained from preprocessed images by means of classification algorithms. Fig. 14 shows the image acquisition system.

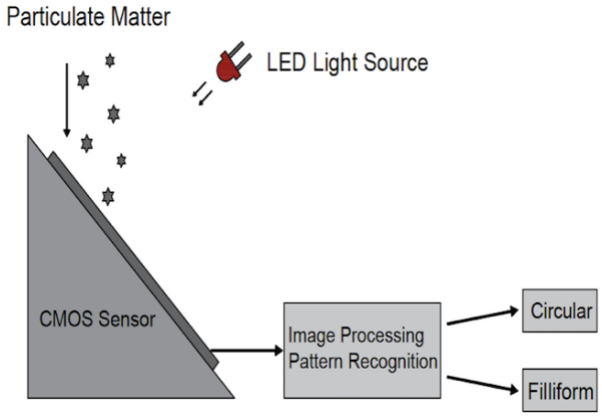

Figure 14. Dust sensor setup based on deposition on the CMOS camera

4.2.3. Holographic particle counter

A new holographic particle counter (Fig. 15) can determine the number concentration of the aerosol particles in the lower micrometer-sized [117]–[119]

As discussed before, one of the significant limitations of the commonly used light scattering-based devices is the rise of the probability of particle coincidence in the high-density area [120]. As an attempt to fill the gap, a 2D camera sensor instead of a single photodiode can be employed to detect the full 3D information of sensing volume.

In the particle imaging unit, every single particle goes into the sampling channel and exposes to the low power diode laser beam. It diffracts the incident beam and creates the circular interference fringe pattern in the detection plane. The particle number concentration can be obtained using pattern recognition on the recorded images [121].

Fig. 15 shows the complete geometry of the holographic particle counter. The proposed setup can attach to the Condensation Nucleus Magnifier (CNM), which works based on the

principle of magnifying the small particles before exposure to the laser light. Therefore, the system is intended as an acceptable alternative to condensation particle counters (CPCs).
The benefit of this configuration is that it does not require a narrow inlet for counting each particle in the observation volume, and it is independent of the speed and direction of the particles.

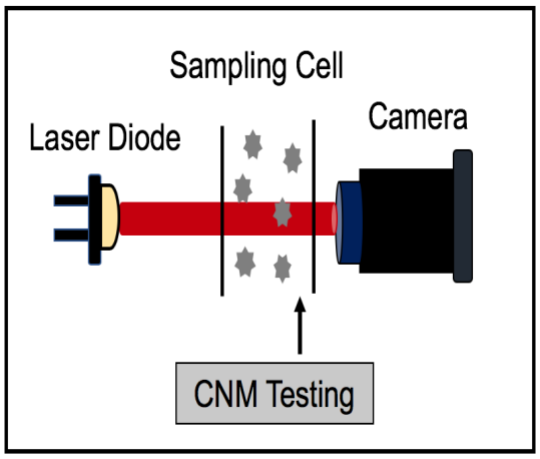

Figure 15. Holographic optical counter

4.3. Comparison and Discussion

Table 7 shows the measurement specifications of the newly designed camera-based optical particle sensors for air quality monitoring (e.g., the typical detection range of the PM based on functional operation, the different structures, and other limitations of the sensors).
The low-cost and simple design COMS image sensor is able to provide detailed information on the shape of the particles in addition to their size. In this framework, it is possible to identify dust origins. It should be noted that the sensor can be efficiently used for the fixed indoor environment such as museums or cleanrooms.
As is evident, the mobile filter-based sensor using wide wireless connectivity seems a promising candidate for low-cost PM monitoring. However, the sensor still needs some improvements in terms of the sampling system, detection size range ,and dimension.
Among the others, the holographic particle counter seems a compelling alternative to the condensation particle counter (CPC) for determining the airborne particle number

concentration of lower than μm- rang. The sensor enables not only accurate measurement of the low particle number concentration but also allows determination of higher particle densities.

Table 6. Comparison of camera based PM sensor

Sensor Type	Holographic based sensor	Filter based sensor	CMOS sensor
Working principle Image	Holography + Image processing	Image processing	Image processing
Size fraction	PM above 3-4 μm after condensation	PM above 3μm	PM above 3μm
Minimum Resolution	Single frame :4.16 ($\frac{\neq}{ccm}$),20fps:0.208 ($\frac{\neq}{ccm}$)	-	-
Detection system	Number Concentration	Size detection / Mass concentration	Size detection/Shape
Reference system	TSI-3775 Commercial	Particulate monitoring station	-
Light source Laser	diode (635nm)	3RGBLED 1 IR LED 1 UVLED	White LED
Detector	UI-3082SE-M Camera IDS(COMS sensor)	RPI NOIR Camera V2	Life Cam HD-3000 (COMS sensor)
External Lens	-	Macro Lens 15×	Without lens segment of camera
Dimension	Small (Without CNM)	Small	Small

This chapter reviews the development and current status of newly designed optical camera-based sensors for real-time PM monitoring. The proposed techniques appear very promising

for the development of the PM air monitoring sensors, but there are still some issues with the increasing of the detection size of the particles as well as their accuracy.

Since demands for such a system considerably increase, we can estimate that new and more accurate devices based on new structures and processing methods may appear in the near future.

However, the use of 2D camera sensors instead of single-pixel photodiodes is a concern for using the proposed sensors after vehicle tailpipe.

It is expected that the high temperature of exhaust emission can affect the vehicle tailpipe, so it is necessary to use a dilution system before the sensor.

In addition, one of the main concerns regarding the use of the 2-D camera based sensors after tailpipe can be related to increasing noise in the detection process of the camera due to tailpipe vibrations.

Chapter 5: General overview of the optical particle counter structures and principle

5.1. Mie theory:

The Optical particle counter principle is based on light scattering methods. For the electromagnetic scattering of a spherical particle, Mie theory and Rayleigh theory as the analytical solutions of Maxwell's equations, depending on the different particle size are suitably used [56]. Both theories are considered as elastic scattering theory when the incident light and scattering light are in the same frequency range[56]. They model the scattering of the electromagnetic radiation by a single particle in a homogeneous medium [122].

The theory behind the scattering of light was initially developed in the 19th century (Mie 1908), while the first modern OPC was developed in the 1940s [123]. Light scattering occurs when a spherical particle with a particular size prevents the direct transition of the incident light and redirect photons into new directions [124]. According to Mie scattering model, the intensity of the scattering light I_s depends on several factors, such as the size parameter x, the refractive index of the particle n and the scattering angle between the incident light and scattered beam light θ, so that the intensity of scattered light can be defined as $I_s = f\ (x, n, \theta, d)$. The size parameter x can be expressed as $x = 2\pi r/\lambda$ [56]
where r is the particle length (radius) and λ is the wavelength of the incidence light. Mie theory is usually valid when the size of particles is comparable to the wavelength of light, i.e. $x = 1$. Generally, when the particle size is much smaller than the light wavelength, i.e. $x \ll 1$, Mie theory converges to Rayleigh scattering. For $x \gg 1$, Mie scattering theory gradually converts to geometric optics with the increase of particle size.

Optical particle counters measure the concentration of airborne particles in ground-based or balloon-based atmospheric studies. Non-spherical soot particles contained individual spherules, are usually exist in atmosphere [125]. These soot aggerates create from the combustion process (e.g., Diesel engines). Non-spherical particles usually define by equivalent diameter, which is the diameter of the spherical particle ,defined as the equal size measurement of the particle under consideration. Assuming the dust particles as a spheres, laboratory measurement was in good agreement with the theoretical modeling of scattering properties of non-spherical particles by the use of Mie theory [126].

5.2. Scattering intensity for a single particle:

When the monochromatic plane wave illuminate a spherical particle, the intensity of the light scattering of a single particle shows in the following equation.

$$I_s = \frac{\lambda^2 I_0}{4\pi^2 R^2} \left(|S_1|^2 sin^2\varphi + |S_2|^2 cos^2\varphi\right) \quad (2)$$

where, λ is the wavelength of light source, I_0 is the light intensity, R is the distance between observation point and particle, S_1 and S_2 are the amplitude function linked to scattering angle of θ (the angle between the direction of light beam propagation and scattered light). In addition, φ stands for the angle between the vibration plane of incident light and scattering surface.

5.3. Structure of optical particle counter:

Figure 16 shows the overall structure of the optical particle counter. A constant-flow pump makes the sampled particulate matter to flow through the optical sensor chamber and finally exits from the outlet pipe. Inside the sensing chamber, an inlet nozzle directs the flow close through the accumulated laser beam. The round inlet sampling pipe of the OPC is designed in a way that the laminar flow through the sampling pipe is guaranteed.

Generally, inside the measurement chamber, the laser beam is accumulated by different lens or mirrors. Variety of lasers with different wavelengths can be used in the measurement chamber to accommodate more particle size. The incident light is scattered in all directions while the exhaust emission is illuminated by accumulated laser source. A simple photodiode can be placed orthogonal to the laser light to detect the intensity of the scattered light.

However, any dirt inside the sensing chamber can change the inner surface reflectance and increase the amount of stray light. Since the scattered light from particulate matter is weak, suppression of stray light components by the use of light trap is important issue.

In the control circuitry, the resulting signal is amplified using a preamplifier and then converted into a digital signal to be processed. It is worth mentioning that the considered diameter of the collimated laser beam is slightly wider than the inlet nozzle diameter. In this way, each particle is fully illuminated when passing through the laser beam.

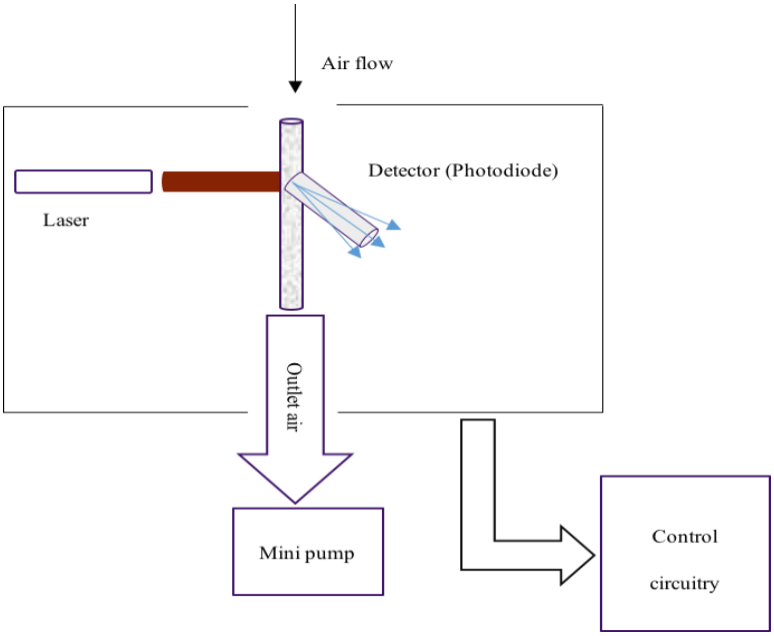

Figure 16. Structure of the OPC

There are a variety of mobile optical PM monitors available in the market. the first group of sensors (Fig.17) uses a heating resistor, that aims to create a thermal updraft [127]. However, the use of a resistor for heating the sample air can limit the possible operation condition (e.g., the power consumption and response time of the sensor will be higher). Besides, it is not possible to have a strict orientation during sensor operation [127].

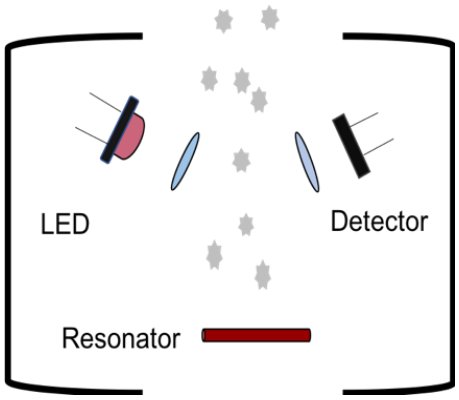

Figure 17. Layout of the sensors which use a heater resonator

The second group of OPCs (Fig.18)include a small, constant-flow pump or fan that regulates the airflow[128]. Generally, when the pump (fan) operates, the airflow enters the inlet duct and passes through the sensing chamber. Finally, the sampling air goes out from the outlet duct of the sensor. The inlet airflow velocity is set to V= 1.2 m/s, the average air velocity entering the human nose during inhalation. The main advantage of these OPCs is that they are fast response and usually work in low-power consumption.

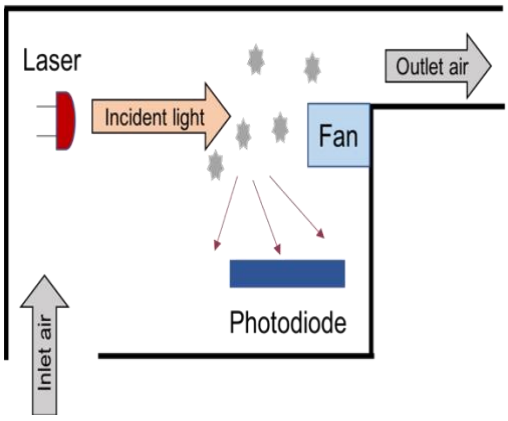

Figure 18. Total structure of OPCs including fan (pump)

5.4. Observation volume of sensing cell in OPC

The volume of observation can be identified at the intersection of the laser light beam and the sampling pipe and is characterized by a cylindrical shape. The sensing volume orthogonally placed with respect to the photodetector and the presence of a single particle in observation volume is a common assumption that is applied for optical particle counters [129]. Since the final aim of the equipment is to detect the real concentration of the particulate matter, it should be assumed that one particle passes through the observation volume at a time. If D is the laser beam diameter and d is the diameter of the inlet nozzle, the observation volume or volume of the sensing cell V_s can be determined as follows :

$$V_s = \pi \frac{d^2}{4} D \tag{3}$$

Diode lasers and high-power LEDs can be used as a light source within the optical particle counters. The use of LEDs does not guarantee a collimated light because they are designed for wide radiation angles. However, even if the diode laser beam diverges as a results of diffraction, the requested beam diameter w_l can be obtained by using suitable lenses after the laser.

Assuming the same exhaust concentration for the sampled emission, the maximum concentration C_m of the sampled exhaust emission in the presence of one particle inside the observation volume can be expressed by:

$$C_m = \frac{1}{V_s} \tag{4}$$

where C_m is expressed in terms of $particles/m^3$. The previous formula shows that always exists a limit to the maximum concentration depending on the observation volume size.

Besides, it is assumed that $C \leq C_m$ holds in the presence of one particle in the observation volume.

In fact for a particle concentration of $particles/m^3$, CV_s determines the expected number of particles in a volume V_s. Considering p as the probability to find one particle in the volume of observation ,if $C \leq C_m$, therefore

$$p = CV_s \ll 1 \tag{5}$$

Figure 19 illustrates the particle sensor layout in which observation volume corresponds to the intersection of the cylindrical from the duct with cylindrical laser beam light.

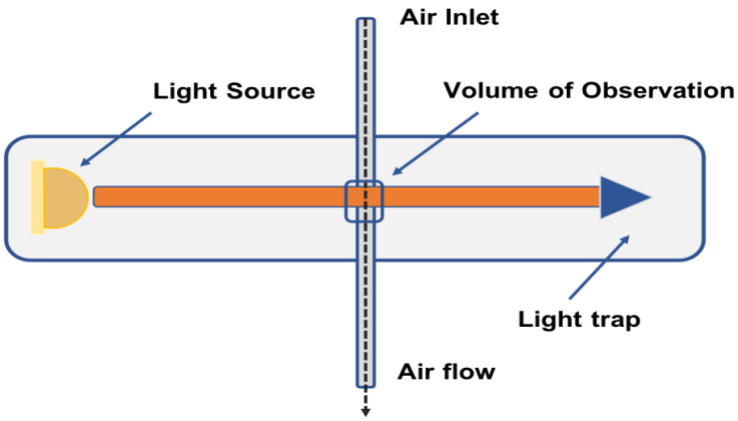

Figure 19.The Schematic of the sensor Observation volume

5.5. Probability of coincidence

Optical particle counters are widely used in science and in the industry to detect particle mass and number concentration. As seen before, by assuming the presence of one particle in the observation volume at a time, it is possible to estimate the each particle size by analyzing the signal received by the photodiode. Considering the size detection of the particle, one of

the principle errors of the OPC is coincidence of particles, which is the simultaneous presence of several particles inside the observation volume.

A theoretical method to explore the effect of coincidence error on the measurement results of optical particle counters descried by Raasch and Umhauer (1984) [130]. In this theory, particles are assumed as point masses with no preferred position and no interact with each other while they pass through the observation volume . Figure 16 shows the coincidence error in the sensing volume of the optical particle counter.

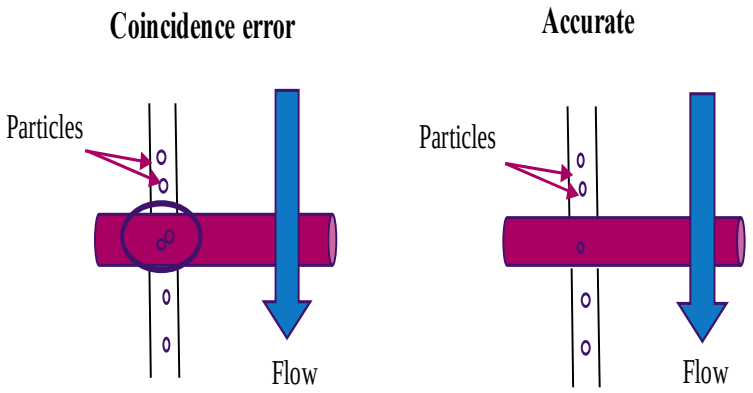

Figure 20. Coincidence error and accurate measurement in observation volume

From Figure 20, it is clear that, during the detection process, the photodiode records the same signal regardless of the actual number of particles. Therefore, the presence of more than one particle in the observation volume causes an underestimation of the real number concentration of the particulate matter. The particle size distribution can shift toward larger particles, as several particles in the observation volume may be detected as one larger particle.

Whitby and Willeke (1979) expressed [131] this error and suggested that it may be decreased by reducing the observation volume or by diluting the sampling particle flow to the OPC. Both of these techniques are analyzed in this research, and it is selected the best solution for using the OPC after exhaust.

The probability of coincidences depends on the average number μ of particles inside the observation volume. By measuring the number concentration N, the average number of particles in the sensing volume is given by :

$$\mu = N \,.\, V_s \tag{6}$$

Generally, coincidence is not of concern when the number concentration of the particle is low. The probability of the presence of several particles in observation volume increases with the particle number concentration. To avoid coincidence of particles, there should be a limitation for the maximum number concentration of sampled emission. In fact, the coincidence error limits the upper number concentration of the optical particle counter.

Assuming a random distribution of particles in the flow, the probability P_k of a simultaneous finding of k particles at the same time in observation volume can be defined by the Poisson distribution[131]:

$$P_k = \frac{\mu^k e^{-\mu}}{k!} \tag{7}$$

When a particle transits through a laser beam, it is possible to define the duration Δt of the signal recorded by the photodetector, and the time interval $\Delta t'$ elapsed between two successive particles entries into the measurement chamber. If $\Delta t' \leq \Delta t$, different forms of signal superposition can occur (e.g. due to the simultaneous presence of two or three particles in the observation volume, the resulting signal is given by the sum of the individual signals associated to each particle). Conversely, if $\Delta t' \gg \Delta t$, the successive light scattering signals do not overlap [132].

5.6. Laminar flow in the optical particle counter sampling:

One of the main parameters to describe the laminar flow in OPCs is the Reynolds number. For the flow in a pipe, the Reynolds equation [133] is:

$$Re = \frac{\rho D\ v}{\vartheta} = \frac{Dv}{V} \tag{8}$$

where Re is the Reynolds number, ρ is the density of the air flowrate, D is the diameter of the inlet sampling, v is the air flow rate, and $\vartheta$is the dynamic coefficient of viscosity. In particular, laminar flow and turbulent flow[133]occurs when $Re < 2300$ and $Re > 2900$, respectively. If the Reynolds number is larger than the critical value, the flow is not stable .

This is a crucial point to be considered, because the instability of the inlet sampling probe flow could negatively affect the detection accuracy of the system. Therefore, the inlet sampling probe should be adequately designed to guarantee laminar flow conditions according to the Reynolds equation.

5.7. Temperature effect on optical particle counter

The condition of the diluted exhaust emission in the inlet probe of the measurement chamber, in terms of temperature , is one of the primary issue for the measurement process of OPC. To address the problem of large size and high-cost, many optical particle counters with diode laser as the light source were developed.

However, the functional characteristics (e.g., wavelength) and operating lifetime of the diode laser can change considerably with temperature. Since the OPC is calibrated using the known particles with the constant laser wavelength, any temperature instability can affect the system detection accuracy. In addition, diode laser lifetime and performance is influenced by the temperature. As an example, by operation of a laser diode at 10 ℃ above the rated temperature, the diode life [134] is decreased by half. In this framework, the temperature of the inlet OPC should always remain in the operating range of about -10 ℃ to 50 ℃.

5.8. Humidity effect on optical particle counter

The behavior of the optical particle counter based on the concept of light scattering can be influenced by humidity in various ways. One possibility is the change of its performance [135] due to the dependency of the particle refractive index on relative humidity.

Secondly, humidity can affect electrical components by creating resistive bridges between each of them [135]. Thirdly, the hygroscopic growth of the particles (like sodium chloride) with the relative humidity increase, causes a significant large positive artefact in particle mass measurement [136]. In addition, if the humidity is about 100%, it is likely to detect liquid droplets as particles, downgrading the accuracy of the detection system. The particles mass and number concentration can be overestimated while the relative humidity is in the range of 70% - 75% [135], or even 60% [137].

However, the relative humidity inside the measurement chamber is not the same as in the sampling probe before the optical sensor. The reason is the increase of temperature inside the chamber due to the electronics circuits during the OPC functioning [138]

Chapter 6 :

Design of the PM sensor after exhaust vehicle

6.1. Structure of particle sensor for detection of PM after exhaust

In order to detect the particle from vehicle diesel exhaust, it is necessary to design the detection system . Considering the main goal of the research which designing the PM sensor based on light scattering, the general layout of the measurement system is composed of three main units (Figure 21):

A- Particle sampling unit

B- Particle sensing unit

C- Signal processing unit

The particle sampling unit consist of PM gas pump and purge air that allow the air to purge the probe and prevent the PM coated on optical components. The air flow rate should be much lower than exhaust flow rate at measurement point to have minimal impact on the detection process of the sensing unit.

The particle sensing unit as a main body of the sensor comprise light source, lenses and detector. In order to decrease the reflection of the scattered light inside and outside of the sensing unit should paint with black matt varnish. To minimize the effect of stray light, a light trap should construct on the right hand of the main body to suppress the stray light.

The signal processing unit is primarily a current to voltage converter. The weak current from the photodetector amplify using the low-noise amplifier .The high pass filter and a 50 Hz notch filter can be used to remove power supply noise and stray light voltage respectively. Finally, the transmission power collected by the photodetector is analysed by the data acquisition system.

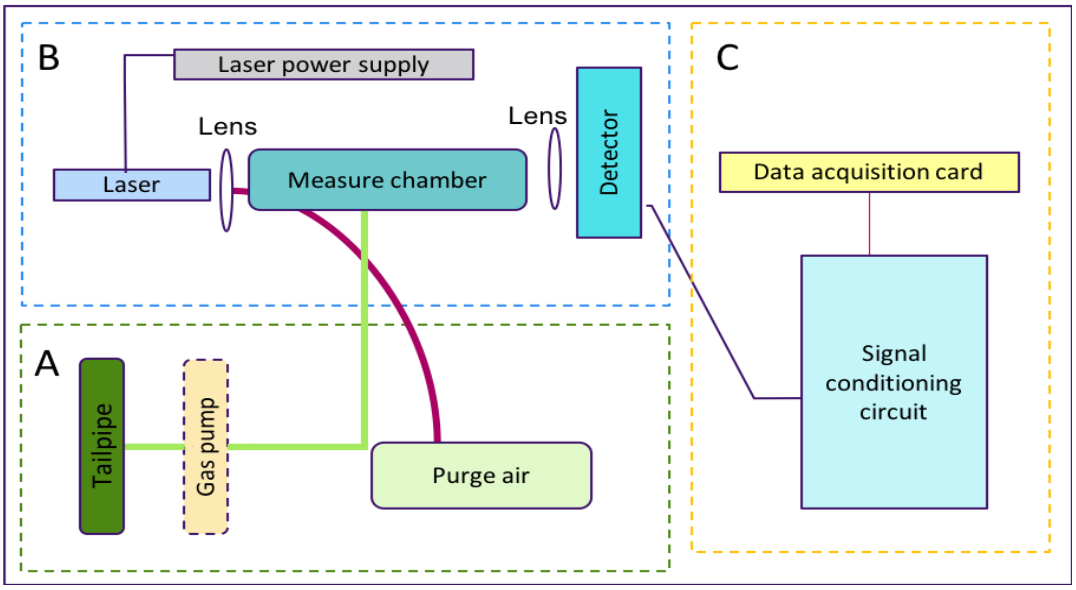

Figure 21. Total structure of the PM measurement system

6.1.1. Particulate matter number and gas flow rate

In the sensing unit, the output signal of the detector is directly related to the exhaust gas flow. In fact, the higher sampling air flow rate contribute to the more detected signals by the photodiode.

There are two ways decrease and control the air flow rate in the sampling inlet pf the OPC.

1. Measure flow rate by access to the ECU and correct the signal accordingly

2. Having constant flow rate by using a gas pump for sampling emission

The first method is less reliable, and it needs complicated computations. Besides, by the use of this method, the PM sensor response will be relatively slow. The second technique is more accurate, and the pump is available on the market at a reasonable cost.

6.2. Sensing unit in optical particle counter:

In order to detect the particulate matter concentration after vehicle exhaust, designing the compact and low-weight detection system is important issue. In this framework, it is necessary to choose the appropriate components of the sensing unit at reasonable cost. In the next step, the best arrangement of the optical components can lead to maximum detection accuracy and compact structure of the instrument. The total aim of this optical setup is the detection of the mass and number concentration of the particulate matter in the real-time.

6.2.1. List of component of the PM sensor:

1- Light source:

It is necessary to select a laser diode as a light source in the visible range spectrum (usually stated to be in the wavelength of 400 nm to 700 nm) and by the power of 5 mW to 100 mW. The diode laser with higher power has the advantage of higher scattered intensity received by photodetector but there is always the increasing of the noise in the detected signals. The priority for choosing the light source is the laser with lower power to avoid any extra noise in detection system.

2- Photodetector: To detect the scattered light from particles, simple pin photodiode is used. The photodiode is polarized in photovoltaic mode to maximize the amplifier sensitivity. The system collecting the light scattered in orthogonal direction to the incident light. In the orthogonal direction, for small particles, scattering light intensity attenuates quickly as a function of the particle diameter, so the particle resolution will be better than nearly forward direction. Secondly, it is likely to eliminate the optical noise for the incident light perpendicular to the detector surface. Therefore, the orthogonal direction of the photodiode respect to light source seems the most promising angle to collect the scattered light.

3- Spherical Lens or mirror: Lasers produce highly coherent light which always diverge to a certain degree. The beam divergence defines how much the light beam spreads out over increasing distance from the optical aperture. Two spherical lenses in parallel should use to collimate the laser beam into the appropriate size range. The first lens applies to make the laser beam parallel, while by using the second lens, the height of observation volume can be defined.

6.2.2. Applying the first lens after the laser light

In order to prevent laser beam divergence, the first spherical lens directly use after the laser light to have a parallel beam (Figure 22). The diameter of the laser after using the first lens can be calculated using the following formula.

$$X = 2Y \tan\left(\frac{\theta}{2}\right) \tag{9}$$

where X is the diameter of the beam after lens, Y is the distance of lens from laser and θ is the divergent angle of the laser.

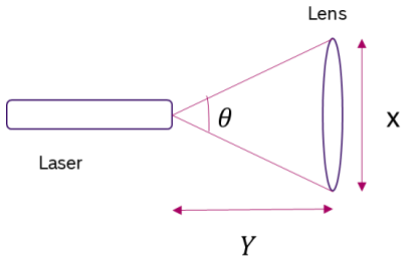

Figure 22. Using the first lens after the laser to have a parallel laser beam

Figure 23 shows the diameter of the laser beam after first lens vs distance from the laser.

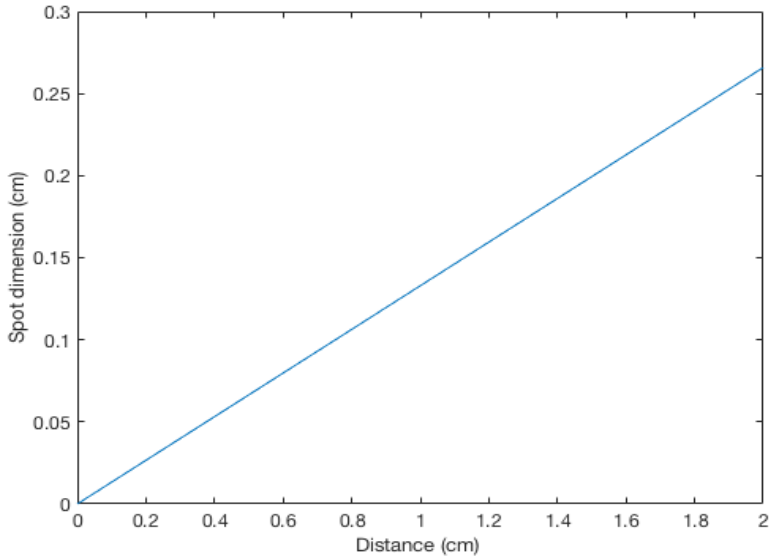

Figure 23. Spot dimension of the beam vs distance from light source

6.2.3. Applying the second lens after the laser light

To collimate the laser beam, we need to decrease the diameter of the laser beam after the first lens. Second spherical lens is used to reduce the spot size for defining the appropriate observation volume of the PM sensor. Figure 24 shows the total configuration of system after using two lens.

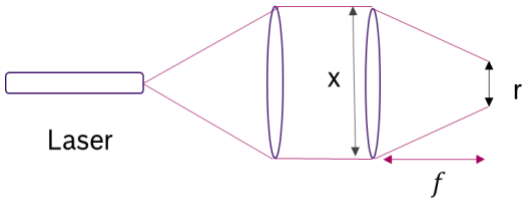

Figure 24. Using the second lens after optical system

The diffraction limit is defined by $\theta = 1.22\left(\frac{\lambda}{X}\right)$, where λ is the wavelength of the light, and X is the dimension of the laser beam before second lens. The factor, 1.22 comes from the circular geometry aperture.

Considering $r = \theta * f$, r is the spot size dimension after the second lens, and f is the focal point of the lens. Therefore, the dimension of the focused light, can be defined as the following formula:

$$r = 1.22\left(\frac{f\lambda}{X}\right) \tag{10}$$

Figure 25, shows the diameter of the laser before the second lens vs spot radius. The wavelength of the light and focal length of the lens are chosen, 400 nm and 20 respectively. As the size of the spot after the second lens in the focal length is too small, it is needed to define the volume of observation after the focal length. It means that the intersection of the inlet duct with laser beam should be after the focal length of the second lens.

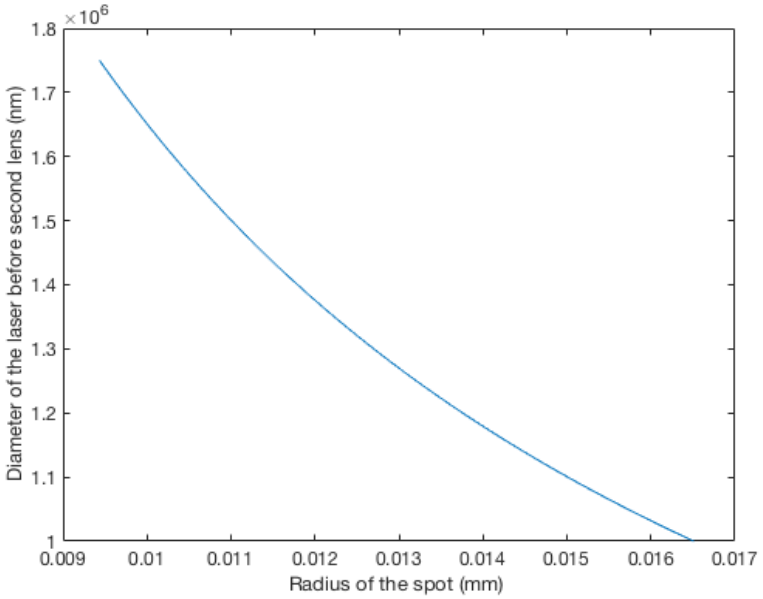

Figure 25. Diameter of the laser beam before the second lens vs spot size in the focal length

The dimension of the spot after focal length of the second lens can be considered as follows:

$$d = \frac{af}{X} + f \tag{11}$$

where a is the diameter of the laser beam after focal length of the second lens with the distance of d from the second lens. The focal lens of the second lens f is 2 cm.

Figure 26 shows the distance of the laser spot from the lens vs laser diameter before the second lens. It should be mention that, the final diameter of the spot for defining the observation volume is chosen 2 mm. In the following section, the total geometry of the observation volume is presented.

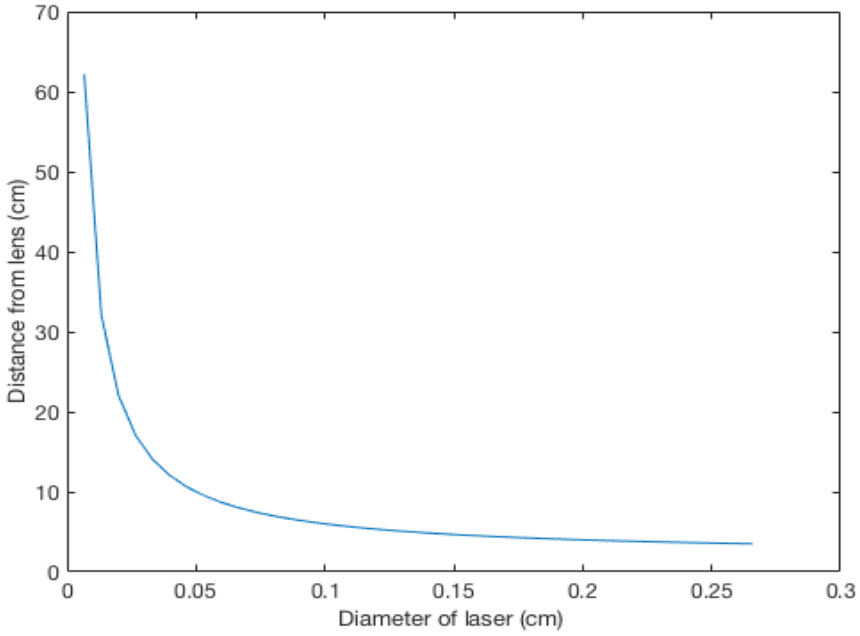

Figure 26.Distance from the second lens vs diameter of the laser

6.3.3. Total dimension of the sensing unit

The minimum distance from the light source to observation volume by the use of two spherical lens is about 7 cm .However, the final length of the sensing unit including the laser diode and light trap is assumed about 10 cm to 12 cm. Figure 27 shows the total configuration of the PM sensing unit (12 cm. 7 cm)

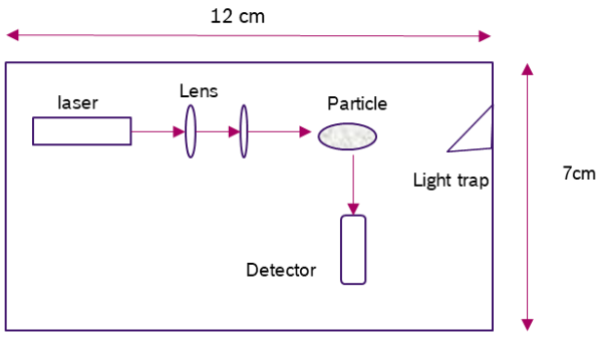

Figure 27.Total structure of the optical sensor detection system

Chapter 7 :Monitoring of particulate matter concentration after exhaust using OPC-N3

7.1. Selecting the optical particle counter in the market

As the second solution instead of developing the new optical PM sensor, it is decided to use one of the current commercial OPC in the markets. A wide variety of low-cost optical particle sensors from different companies (e.g., Dylos, AlphaSense, TSI) is available on the market. Among them, OPC-N3 sensor produced by AlphaSense Company, which is commonly used for air quality monitoring is characterized by a good compromise between cost and accuracy. Table 8 summarizes the main characteristics of the OPC-N3. However, since the minimum detection size of the OPC-N3 is 0.35 μm, the focus of the proposed research will be mostly on accumulation mode rather than nucleation mode.

There are several exhaust emission particles in the nucleation mode, which OPC cannot detect. However, it is not a concern, while we focus on the particulate matter mass concentration (accommodation mode) to determine the DPF performance.

Accumulation mode contains solid carbonaceous particles resulting from incomplete fuel combustion. The size and number of the accumulated particles depend on the combustion process, fuel oxidation, condensation of species, etc. [139].

Table 7. OPC-N3 technical specification [140]

Technical Data	**OPC-N3**
Number of bins	24
Size range (μm)	0.35 to 40
Total flow rate (l/min)	5.5
Temperature range (℃)	-10 to 50
Humidity range (%rh)	0-95
Max coincidence probability (Concentration at 10^6(particles/lit))	0.84
Max coincidence probability (Concentration at 500(particles/lit))	0.24
Weight (g)	< 105

The Grimm aerosol sensor provides an excellent capability for detecting the particulate mass concentration by using the light scattering method [141]. The sensor is compact,

durable, and require only a minimum of maintenance. The accuracy of the OPC-N3 sensor compared to the Grimm sensor under the environmental condition constant is as about 11% to 14% over the range of PM1.0 mass concentration. The sensor accuracy also slightly increases (16% to 24%) with rise of PM2.5 mass concentration[142]. Generally , for the both values, the concentration of the PM at 20 °C and 40% relative humidity greatly underestimate [142] in comparison with the GRIMM sensor.

The concentration of the particulate matter emission from the tailpipe, even if using DPF, is still too high to an accurate detection by optical particle sensor . However, for using the OPC-N3 after exhaust, it is necessary to consider the single- particle detection in the observation volume. In this framework, two main solutions: 1) diminishing the observation volume and, 2) diluting the raw exhaust with ambient air will be investigated.

7.2 . Reduction of observation volume (First solution):

Accurate detection of the size distribution requires a low coincidence error, which can be obtained by reducing the volume of observation.

Considering that the maximum real number concentration of the diesel engine for the particle of 0.35 μm is about 500 $(1/cm^3)$ [143], it is possible to estimate the dimension of the volume of observation required to obtain the flow of one particle at a time. Fig 24 shows the relationship between concentration and diameter of the inlet sampling emission to have one particle in the volume of observation. For the defined cylindrical volume of observation, it is assumed that the diameter of the laser w_l 0.5 mm bigger than inlet duct diameter. In fact, the maximum measurable concentration is limited by the minimum diameter of the observation volume that can be realized. Considering the maximum value of concentration, about 500 $(1/cm^3)$ shown by Fig 28, the needed reduction can be achieved with an inlet duct diameter of 0.121 cm.

To obtain the proposed observation volume, the diameter of the laser beam should be reduced to the value of 0.171 cm, which is simply achieved by using different lenses. The main problem is that the difficulty in building an inlet duct satisfying the requirements, thus a solution consists in diluting particulate matter after exhaust with purge air.

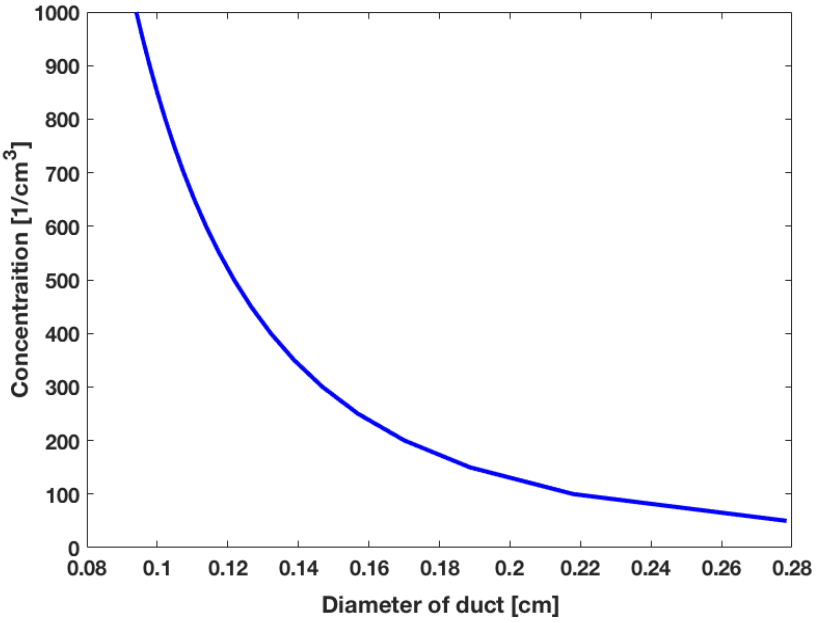

Figure 28. Number concentration vs the inlet duct diameter

Table 8 shows maximum coincidence probabilities of 0.84 and 0.28, and maximum particulate number concentrations of 1000 $(1/cm^3)$ and 0.500 $(1/cm^3)$respectively. For a number concentration of 500 $(1/cm^3)$ the probability of coincidence is still too high while the determination of the exact size of particulate matter is one concern of the detection system.

7.3. Dilution of the exhaust emission with the ambient air (Second solution):

As a second solution to use the OPC-N3 after vehicle exhaust with high accuracy, diluting the raw exhaust with air is proposed. However, to decrease the system cost, it is decided to use the filtered ambient air as a diluter.

Therefore, the best solution to reduce the coincidence error is to decrease the number concentration of particulate matter to the feasible value of around 60 $(1/cm^3)$, which can be obtained with a dilution factor of 8 using eq. (12). The real and diluted concentration can be expressed using the following formula:

$$C_r = DF.C_d \qquad 1< DF < N \qquad (12)$$

where C_r is the real concentration of the exhaust emission, C_d is the concentration of the diluted emission and DF is the dilution factor. The maximum range of the dilution factor can be defined by the requested real concentration and number of the diluters (e.g. ejectors).

7.3.1. Ejector and dilution factor :

Due to their simple design, ejector dilutors are commonly used in exhaust measurement [144], [145]. They work by mixing a limited amount of raw sample emission with a fixed amount of dilution gas or air. There are no moving parts, which ensure a stable and uncomplicated operation over extended time. Another advantage is that pump is not necessary to draw the sample from exhaust emission. Ejector diluters are usually calibrated for conditions where the inlet and the outlet of the diluter are at ambient pressure and temperature. However, the operating functional of these devices shows that the dilution ratio is considerably influenced by sampling conditions.

8.3. First layout for detection the PM after vehicle exhaust

In the proposed design, to decrease the concentration of the sampled emission flow before the optical sensor, particulate matter of exhaust emissions undergoes rapid dilution with ambient air after exiting from the tailpipe.

The suction part of the ejector is connected to the steel tube which is inserted into the tailpipe, while the fluid part of the ejector is connected to the air filter to remove any additional particulate matter entering to the detection system. The use of a single head pump before the fluid part of the ejector is necessary to have a constant flow rate of particulate matter in the mixing zone. Figure 29 shows the overall layout of the detection system using the optical sensor after vehicle tailpipe.

The ejector which placed between the optical sensor and the tailpipe of the vehicle mix the raw exhaust with ambient air.

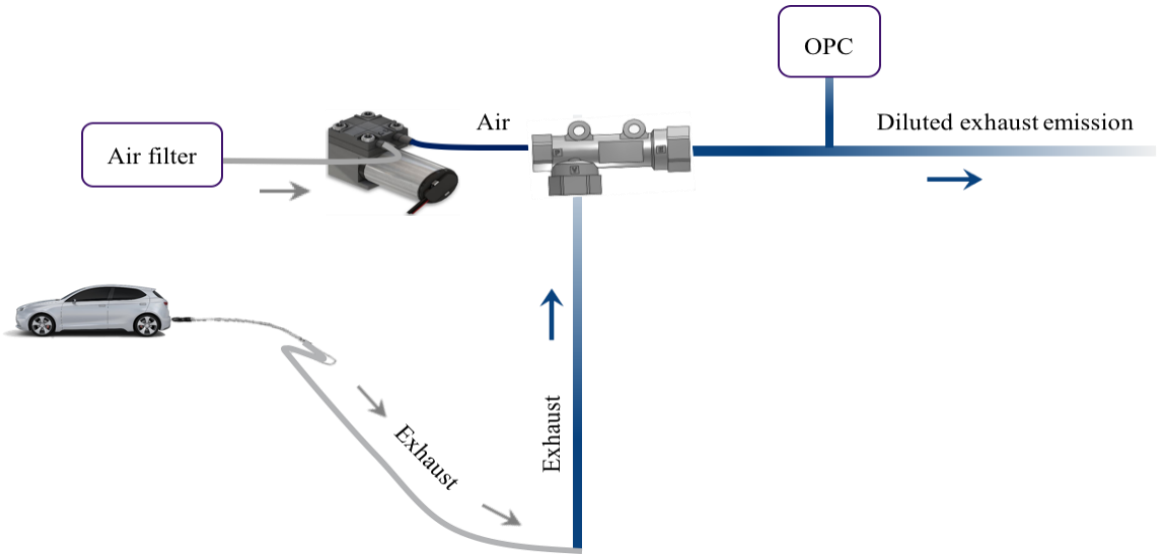

Figure 29. Layout of the system using one ejector for detection of particulate matter

8.4. *Dilution factor for first layout*

The calculation of the total flow rate in mix zone of the ejector for determination of the dilution factor requires the knowledge of the volumetric flow rate in suction part of the ejector (exhaust gas) and supply part of the ejector (purge air). Both of them by using the characteristic curve and selecting the operation pressure of the supply part of ejector can be defined. Among the cheap ejectors available on the market, it was selected the ZH05DSA-06-06-06 ejector with a small throat section of 0.5 *mm*.

Fig 30 shows the characteristic curve of the selected ejector. Different sample composition, temperature and pressure imply the use of ejector dilutors in different locations along the sampling line. Figure 30 is experimentally determined by the SMC company and directly come from [146].

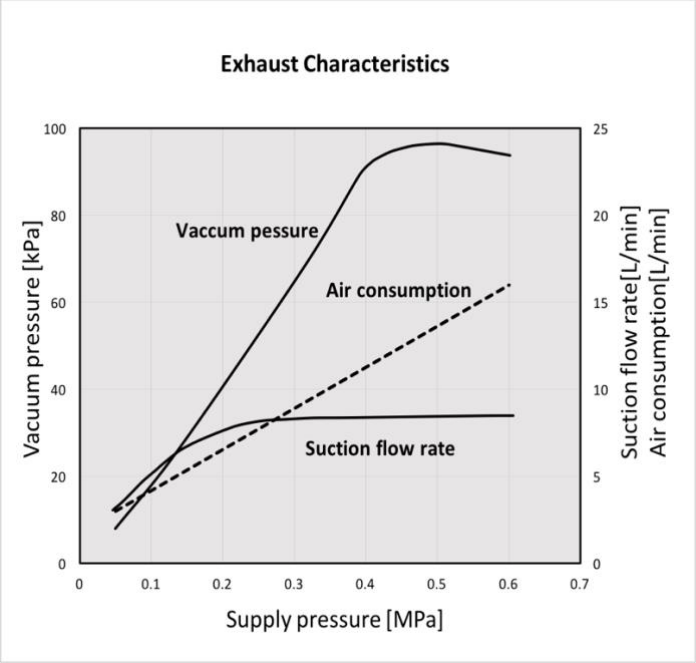

Figure 30. Characteristic curve of the ejector

Table 9 shows the specifications of the compact and light weight ZH05DSA ejector [146].

Table 8.ejector specification

Technical Data	**ZH05DSA-06-06-06**
Fluid	Air
Operating temperature range (℃)	-5 to 50
Operating pressure range (MPA)	0.1 to 0.6
Nozzle nominal size (mm)	0.5
Maximum suction flow rate $(l/\min)$	8.26
Air consumption $(l/\min)$	16
Weight (g)	5

The calculations of the total volumetric flow rate of the mix condition and dilution factor are shown in Table 10. The total flow rate is calculated by the sum of the exhaust and air flow rate with the following formula. The mixed emission before the optical sensor should always remain laminar.

$$Q_T \cdot \rho_T = Q_{exhaust} \cdot \rho_{ex} + Q_{air} \cdot \rho_{air} \quad (13)$$

where, Q_T is the total volumetric flow rate of diluted particulate matter sampling in mix condition, $Q_{exhaust}$ is the volumetric flow rate of raw exhaust in suction part of the ejector, and Q_{air} is the volumetric flow rate of the environmental air in the supply part of the ejector. Here, ρ_T, ρ_{ex}, ρ_{air} are the total density of the diluted particulate matter, density of the exhaust emission, and density of the air, respectively. It should be mention that to simplify the calculation, the total density and exhaust density are assumed to be equal to air density.

Table 9. Calculation of flow rate and dilution factor

Parameter	Values					
Pressure supply(PM)	0.1	0.2	0.3	0.4	0.5	0.6
Flow rate of exhaust($l/\min$)	5	7.5	8.15	8.15	8.15	8.26
Flow rate of air(l/min)	4.25	6.60	8.95	11.30	13.65	16
Dilution factor	0.85	0.88	1.09	1.38	1.67	1.93
Total flow rate after exhaust (l/min)	9.25	14.1	17.10	19.45	21.80	24.26

The dilution factor in Table 10 is defined as the ratio of air flow rate and exhaust flow rate, and is calculated by the following formula:

$$DF = \frac{Qair}{Qexhaust} \quad (14)$$

By looking at Table 10, to achieve the maximum value of dilution factor, it is reasonable choosing a 6 bar relative pressure for the supply part of the ejector. In addition, after setting the dilution factor and choosing the supply pressure of the ejector, the pump operating point

is established based on the given pressure and flow rate. To make ambient air flowing inside the ejector, the pump should be placed before the supply part of the ejector.

Also, by using the proposed layout, the concentration of the exhaust sampled emission decrease, but it is not enough to have accurate detection by OPC. Considering the OPC-N3 technical specification and maximum detectable concentration of particulate matter (0.500 $1/cm^3$) at particle size of 0.35 μm, the coincidence probability is still high for the presence of each particle in observation volume.

In this framework, to increase the dilution factor up to 8, a different layout including more ejectors in parallel for detection of the particulate matter after tailpipe is proposed.

8.5. Second layout for detection the PM after vehicle exhaust

In the proposed layout, all ejectors except the last one, use ambient air in supply and suction part. The fraction of the raw exhaust emission is sucked from tailpipe by suction part of the last ejector. To dilute the exhaust emission with ambient air, a proper operating point is set for the compressor. As previously mentioned, it is chosen based on the selected supply pressure of the ejector and volumetric flow rate. However, it is necessary to use two air filters, before the compressor and the air suction part of the ejectors.

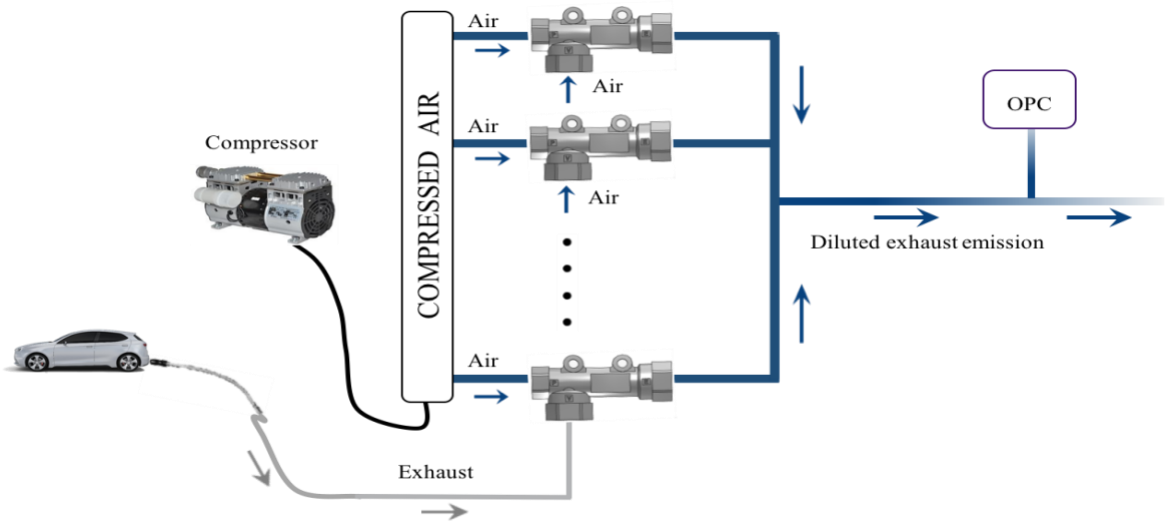

Figure 31. **.** Layout of the system after exhaust using parallel ejectors

In particular, to obtain a dilution factor equal to 8, it is selected a supply pressure of 0.5 MPa based on the characteristic curve of the ejector.The Dilution factor can be calculated by the following formula while the ambient air flows in all the ejectors, except for the suction part of the last ejector.

$$DF = \frac{\sum_{i=1}^{N} Q_{supply\_air} + \sum_{i=1}^{N-1} Q_{suction\_air}}{Q_{exhaust\ gas}} \quad (15)$$

where Q_{supply_air} is the volumetric flow rate of the supply air, $Q_{suction\_air}$ is the volumetric flow rate of the air in the suction part of the ejector, and $Q_{exhaust\ gas}$ is the volumetric flow rate of the emission gas in the suction part of the last ejector. The calculation of $Q_{Total-Air}$, is made as follows:

$$Q_{Total-Air} \cdot \rho_{air} = (n-1).Q_{Total-ejector} \cdot \rho_{air} + Q_{Supply-ejector} \cdot \rho_{air} \quad (16)$$

where $Q_{Total-Air}$ is the total volumetric flow rate of air, n is the number of the ejectors in parallel and $Q_{Supply-ejector}$ is the volumetric flow rate of the supply part of the last ejector. It should be mentioned that in each step, $Q_{Total-ejector}$ for each ejector is the sum of $Q_{suction}$ and Q_{supply} . The supply part of the all ejectors and the suction part of ejectors except the last one contains the airflow. Therefore to calculate the total flow rate of the air, the air density of ρ_{air} was used in the expression 16.

Table 4 shows the total volumetric flow rate, dilution factor, and operating point of the compressor using the ZH05DSA-06-06-06 ejector. In the proposed layout, to obtain a dilution factor equal to 8, four ejectors in parallel are connected. $Q_{air\_compressor}$ presents the final volumetric flow rate of the selected compressor.

Table 10. Dilution factor and flow rate of the second layout

Parameters	values
Number of ejectors	4
$Q_{Total-Air}$ (l/min)	69.66
$Q_{exhaust}$ (l/min)	8.15
DF	8.54
$Q_{air-compressor}$ (l/min)	45.21

The final value of the volumetric flow rate after 4 ejectors is about 69.66 (l/min). By connecting the optical particle sensor to the main tube enables the sampling of a proportion of the exhaust emission to be used in the OPC. The indirect use of airflow allows OPC fan to regulate the flow rate to the appropriate value suitable for the optical sensor (Fig. 32).

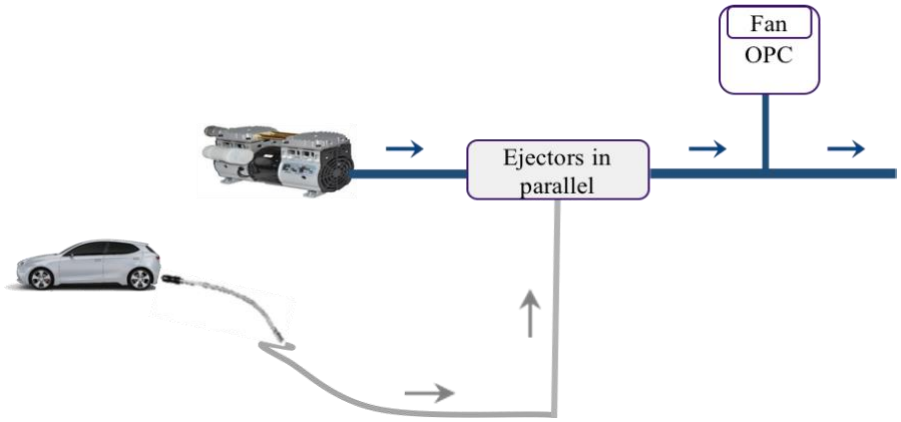

Figure 32. Final layout by OPC perpendicular to the main flow rate

8.6.Total cost of the system

Table 12 shows the total cost of components for designing the proposed sensor. The sensing part of the system is quite cheap (about 340 $). However to increase the accuracy of system and durability , the dilution of the raw exhaust emission with environmental air was proposed. In order to have a simple and affordable prototype, additional sensors (e.g., humidity or temperature sensors) are not used in the proposed system.

Table 11. The component cost of the system

Optical layout	List of components	Numbers	Price
Sampling system	Ejectors and tubes	4	76.6$
	Pneumatic Double Y tube	2	29.42 $
Dilution system	Compressor	1	382.40 $
	Pressure switch	1	51.95 $
	Pneumatic filter	2	218 $
	One touch manifold	1	8.68$
Optical sensing system	OPC-N3	1	340 $
Conjunction system	Accessories	-	90.15 $
Total cost		≈1200 $	

8.9.Calibration process

One prerequisite for using a light scattering based sensor for evaluation of the DPF performance is the availability of the traceable and appropriate calibration method. In order to obtain an accurate measurement, it is necessary to determine the relationship between a scattered light intensity distribution and particle size distribution. A testing setup consists of a generated particle source, reference sensor, and proposed PM sensor.

One possible way to achieve the aim is to use a Standard Combustion Aerosol Generator (SCAG) as a known exhaust source. The particle generator produces real combustion particles with a selected size distribution, which are stable and reproducible [147]. Another commonly used source of the soot particles for calibration of the measurement device is a diesel engine. Generated particles from engine are diluted by the compressed air. The diluted sample passes through the designed sensor (OPC- based sensor) and the reference sensor

(SMPS) sequentially. In order to determine mass concentration of the sampling emission gravimetric method or micro soot sensor can be used. It should be mentioned that the calibration process in the test bench by the use of a diesel engine is time-consuming and relatively high-cost.

Chapter 9 :

Calculation of mixed condition parameters

9.1. Sampling system

Sampling process as an essential part of the sensing system can provide the accuracy and validation of the detection system. The condition of the diluted exhaust emission in the inlet probe of the measurement chamber, in terms of temperature and humidity, is a primary issue for the detection process of OPC. The accurate detection of particulate matter requires inlet nozzle pressure and temperature within the ranges of 1 bar and -10 ℃ to 50 ℃, respectively [140]. Exhaust gas flow rate of the inlet duct is another major issue. To avoid the effect of humidity and vapour condensation on the performance of the optical particle counter, the total relative humidity of the sampling diluted gas should be less than 75% [148].

9.2. Temperature of the Mix Condition (First layout)

One of the most significant factors to be investigated is the temperature of the gas sample at OPC inlet, after the mixing with environmental air in the ejector. The temperature T_{mix}[℃] of the mixture can be calculated by following the adiabatic mixing and the mass balance equations. To calculate the temperature of the gas mixture before the OPC, the ambient air and the exhaust gas temperatures are varied in the range of -10 ℃ to 40℃ and 50 ℃ to 350 ℃ respectively. Fig 33 shows that the temperature before the optical sensor, in different conditions, is mostly less than 40℃ .

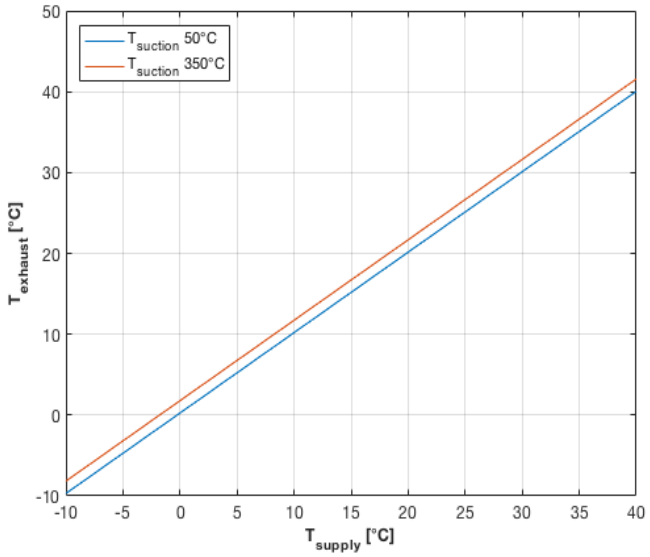

Figure 33.Temperature of the mix condition vs temperature of the raw air

The temperature of the exhaust emission can vary based on the engine operation. In order to evaluate the temperature of the mixed emission before the optical system, it is considered a minimum and maximum temperature for the exhaust emission from 50 ℃ to 350 ℃.

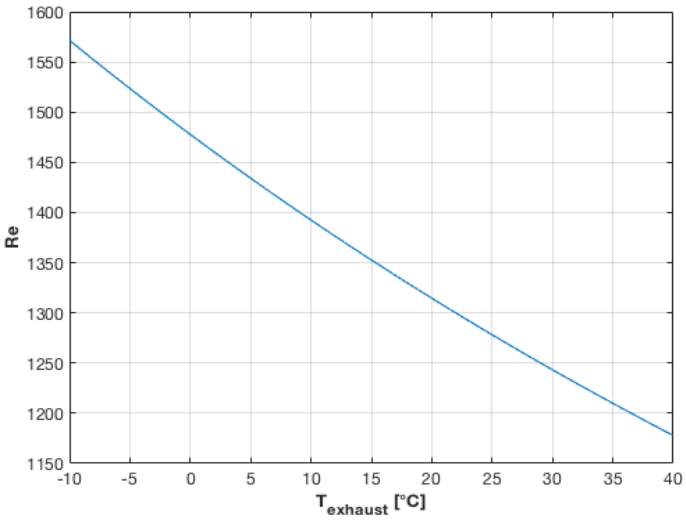

Figure 34.Reynold number vs temperature of mix condition

Generally, the inlet pipe of the OPC is designed with a round section and the sampling emission requires a laminar flow, ensured by a proper value of the Reynolds number (below 2300).

Fig 34. shows the variation of the Reynolds number from the temperature of the mixture flow, which changes between -10 ℃ and 40 ℃.

9.3 Humidity in Mix Condition (First layout)

Humid air can affect the behavior of the optical particle counter based on light scattering principle in different ways. One possibility is the change of its performance due to the dependency of the particle refractive index on relative humidity [148].

Secondly, humidity can affect electrical components by creating resistive bridges between each of them [148]. Thirdly, the hygroscopic growth of the particles (like sodium chloride) with the relative humidity increase, causes a significant large positive artefact in particle mass measurement [136].

In addition, if the humidity is about 100%, it is likely to detect liquid droplets as particles, downgrading the accuracy of the detection system. To avoid the formation of liquid droplets in the sampling probe before the optical sensor, the partial vapor pressure of the diluted sampling emission after ejectors should be always maintained less than saturation vapor pressure, at the mixture temperature. Saturation vapor pressure is defined as the pressure of the vapor when it is in thermodynamic equilibrium with the liquid phase, for a specific temperature. The saturation pressure of the vapor mainly depends on the temperature.

The particles mass and number concentration can be overestimated while the relative humidity is in the range of 70% [148] - 75%, or even 60%[137]. Also, it should be mentioned that the relative humidity inside the measurement chamber is not the same as in the sampling probe before the optical sensor. The reason is the increase of temperature inside the chamber due to the electronics circuits during the OPC functioning [138] .

It should be mentioned that the temperature, pressure, and relative humidity of the environmental air in the supply inlet are assumed to be in the range -10℃ to 40 ℃, 5 bar and 50 %, respectively.

To calculate the humidity after the ejector, the mass of the vapor in the sampled air can be determined by considering the humidity of the environmental air and thus calculating the wet air mixing ratio x.

It is now possible to sum the ejector's air supply mass flow rate with the exhaust gas mass flow rate sampled by the engine, and the water vapor mass flow rate contained in the supply air of the ejector with that contained in the exhaust gases.

Considering these relation, the water mixing ratio of air-exhaust gas mixture (x_{min}) as the ratio of mass flow rate of water vapor in the supply air and in the suction exhaust gases of the ejector ($M_{H2o-tot}$) and the mass flow rate of supply air dry and suction exhaust gases dry of the ejector ($M_{dry-tot}$) can be suitably calculated. Being $P_{STP}$the standard ambient pressure equal to 101325 $[Pa]$, the relative humidity RH can be defined by the following formulas:

$$P_{H2O-mix} = P_{STP} \times 10^{-5} \times \frac{x_{min}}{x_{min} + 0.622} \tag{17}$$

$$RH = \frac{P_{H2O-mix}}{P_{SAT}} \times 100 \tag{18}$$

where P_{SAT} is the saturation pressure of the vapor depending only on the gas mixture temperature. Fig 35 shows the variation of the sampled emission humidity while exhaust temperature varies in the range of 50 ℃ to 350 ℃ . As visible, the humidity at the inlet of the OPC is always less than 35%.

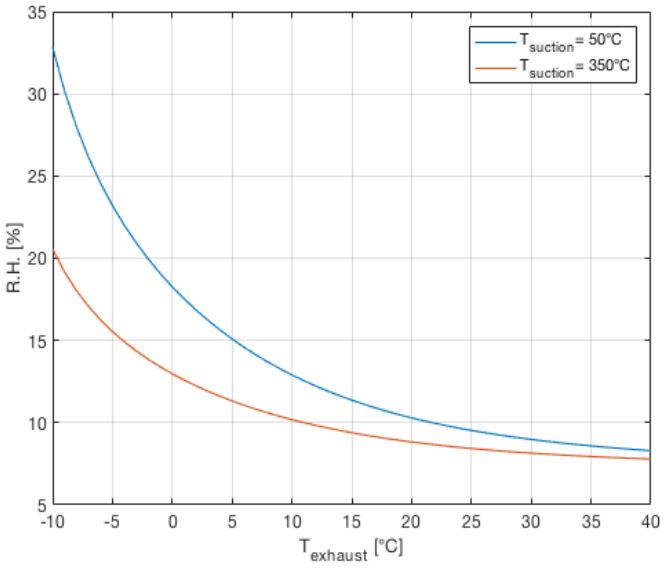

Figure 35.Relative humidity vs temperature of the ejector discharge

9.4. Temperature of the inlet mixture emission of the optical sensor(Second layout)

As highlighted previously, one of the most important factors to be considered is the temperature of the mixture emission after the ejectors and before the optical sensor. To standard working conditions of the optical sensor require a temperature of the sampling emission of the ejectors discharge between -10 ℃ and 50 ℃. The mass flow rate in the mixing point is constant for all temperature and humidity conditions, and can be calculated by the following formula:

$$G_{mix} = G_{suction} + G_{supply} \tag{18}$$

where G_{mix} is the mass flow rate after mixing, $G_{suction}$ is the mass flow rate at exhaust suction, and G_{supply} is the mass flow rate of dilution air. The temperature T_{mix} [℃] of the gas mixture and downstream of the ejector can be calculated considering the adiabatic mixing and mass balance equation to describe the condition before the optical sensor:

$$T_{mix}\, G_{mix} = T_{air-sup} G_{air-sup} + (T_{air-suc} G_{air-suc} + T_{exhaust-suc} G_{exhaust-suc}) \tag{20}$$

where $T_{air-sup}$ is the air temperature in the supply part of the ejector, $G_{air-sup}$is the overall supply air mass flow rate of the four ejectors, $T_{air-suc}$ is the air temperature in the suction part of the ejector, which is equal to $T_{air-sup}$, $G_{air-suc}$ is the air mass flow rate in the suction part of the $(n-1)$ ejectors. Moreover, $T_{exhaust-suc}$ is the temperature of the exhaust emission flowing from the engine to the suction part of the last ejector, and $G_{exhaust-suc}$ is the mass flow rate of the exhaust emission of the engine in the suction part of the last ejector. At each step, the mass flow rate G can be computed as follows:

$$G = Q.\rho \tag{21}$$

where Q is the volumetric flow rate. As an approximation, the total mixture gas and emission sampling density are considered equivalent to the density of air.

To calculate the temperature before the optical sensor in different operating conditions, the ambient air temperature was varied in the range of -10 ℃ to 40 ℃, while the temperature of the engine exhaust gas ranged between 50 ℃ and 350 ℃. Figure 36 shows the temperature of the gas mixture for different operating conditions.

From Fig. 36, it is clear that any change in environment temperature can affect the temperature of the gas mixture after ejector directly. However, the temperature after ejector is less than 50 ℃, and an extra cooler before the optical counter is not necessary.

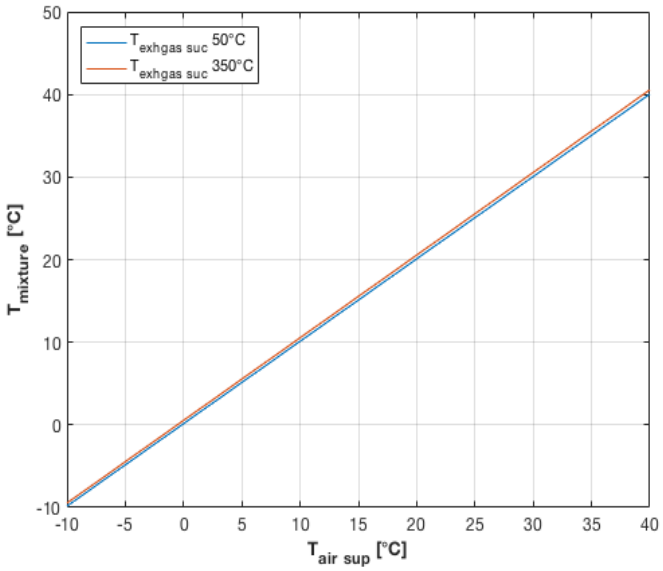

Figure 36.Temperature in mix condition vs ambient temperature

9.5. Measurement of the laminar flow in mixed condition (Second layout)

Using the small pump or fan of the OPC, the mixture of the emission exhaust gas with air flows into the inlet sampling probe, and then enters the observation volume of the optical sensor. In the observation volume, the scattered light intensity is detected by the photodetector, and then the sampled mixture exits from the outlet of the OPC. Accurate measurement of the particulate matter concentration requires a laminar flow of the inlet

sampling of the OPC, ensured by a proper value of the Reynolds number. The Reynolds number must always be less than 2300 to have a laminar flow [133]of the mixture sampling. The total volumetric flow rate of the mixture sampling can be calculated by using the optical sensor technical specifications in Table 1. The flow velocity of the inlet mixture sampling can be calculated using the volumetric flow rate and the inlet diameter of the OPC (6 mm). Finally, the Reynolds number can be calculated given the density ρ of the mixture flow in the discharge of the ejectors (pressure of 1 bar and temperature between -10 ℃ to 40 ℃) and the dynamic viscosity $\vartheta(T)$ of the mixture sampling flow (depending only on the temperature).

Fig 37 shows the dependency of the Reynolds number from the temperature of the mixture flow, which varies between -10 ℃ and 40 ℃. It is worth to note that the Reynolds number is always below 2300, which confirms that the condition of the inlet sampling probe flow is always laminar.

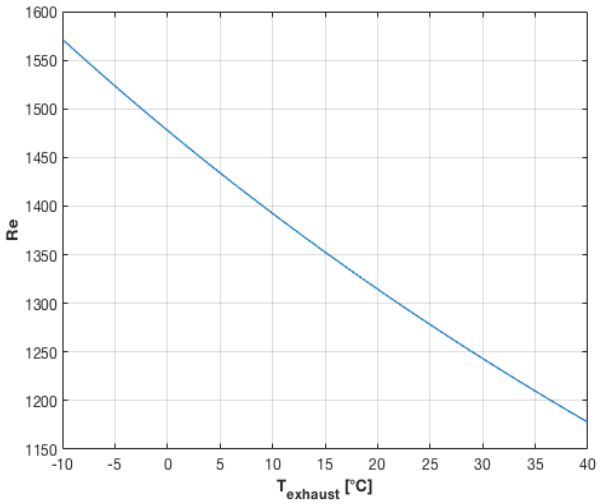

Figure 37.Reynolds number vs temperature

9.10.Humidity calculation of mixed condition for second layout

Humidity can significantly affect the performance of OPCs in various aspects. It is proposed that for the designed layout, the relative humidity of the inlet emission sampling always remains less than 60%.

The first calculation of the vapor partial pressure has been done considering the temperature of the exhaust emission in the range 50 ℃ to 350 ℃ (Fig. 38). For the calculation of the vapor partial pressure and relative humidity after the ejectors, the temperature, pressure and relative humidity of the environmental air in the supply inlet are considered in the range -10 ℃ to 40 ℃, 5 bar and 50% respectively. However, the variation of relative humidity in the environmental air cannot affect the results.

Given the volumetric flow rate of the supply part of the ejector and the density, it is possible to calculate the supply mass flow rate. The mass of the vapor in the sampled air can be determined by considering the humidity of the air, and through the calculation of the wet air mixing ratio x.

Finally, the total mass of the H_2O in the system M_{H_2O-tot} can be calculated formulas follows:

$$M_{H_2O-tot} = M_{H_2O-air-supply} + M_{H_2O-air-suction} + M_{H_2O-gas-suction} \quad (22)$$

where, $M_{H_2O-air-supply}$ is the mass flow rate of water vapor in air supply part of the ejectors. $M_{H_2O-air-suction}$is the mass flow rate of the H_2O in air suction part of the ejectors. $M_{H_2O-gas-suction}$ is defined as the mass flow rate of the H_2O in the sampled exhaust emission that passes through the suction part of the ejector.

To compute the total mass flow rate of the dry air $M_{dry-tot}$, the following formula can be used:

$$M_{dry-tot} = M_{air-dry-supply} + M_{air-dry-suction} + M_{gas-dry-suction} \quad (23)$$

where $M_{air-dry-supply}$ is the mass flow rate of the dry air in the supply part of the ejectors, $M_{air-dry-suction}$is the mass flow rate of the dry air in the suction part of the ejectors, and $M_{gas-dry-suction}$is the mass flow rate of the dry emission of exhaust in the suction part of the last ejector.

Since the total mass flow rate of the dry air and water vapor is known, it is possible to calculate the water mixing ratio of the air-exhaust gas mixture, after ejectors and before the optical sensor, as follows:

$$x_{mix} = \frac{M_{H_2O-tot}}{M_{dry-tot}} \tag{24}$$

To calculate the relative humidity and partial vapor pressure after the ejectors, the values of 350 ℃ and 50 ℃ have been considered for the exhaust emission. Fig 38 shows the saturation vapor pressure and partial pressure of the vapor while the temperature of emission mixture changes between -10 ℃ to 40 ℃.

From Fig. 38, it results that there is no water droplet in the observation volume, while the partial vapor pressure is always below the saturation pressure. The partial pressure of the vapor in mix condition after ejector $P_{H2O-mix}$ can be calculated as.

$$P_{H2O-mix} = P_{STP} \,.\, 10^{-5} \,.\frac{x_{mix}}{(x_{mix} + 0.622)} \tag{25}$$

where P_{STP} is the standard ambient pressure equal to 101325 $[Pa]$. The relative humidity RH can be calculated from:

$$RH = \left(\frac{P_{H2O-mix}}{P_{SAT}}\right).100 \tag{26}$$

where P_{SAT} is the saturation pressure of the vapor depending only on the gas mixture temperature. To avoid any condensation, the partial vapor pressure of the sampling inlet emission must always be less than saturation pressure of the vapor. Figure 39 shows the relationship between the humidity of diluted exhaust emission in the mix condition after ejectors and before optical sensor, for different temperatures of ejector discharge.

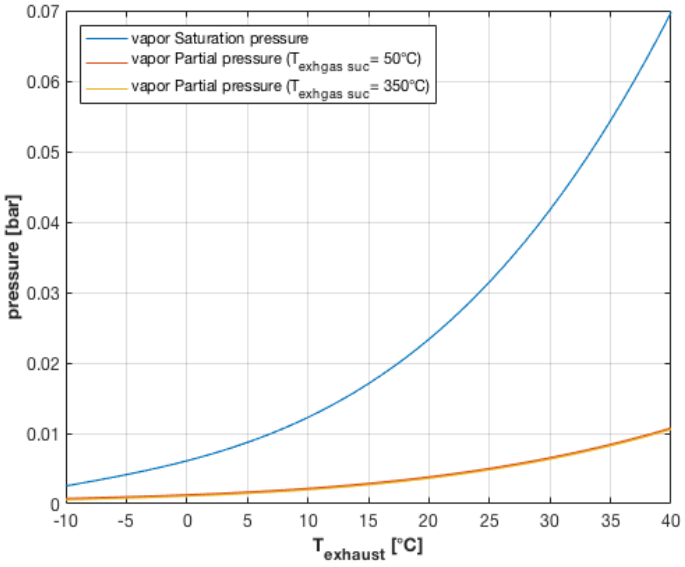

Figure 38. Vapor partial pressure and vapor saturation pressure vs temperature of discharge ejector

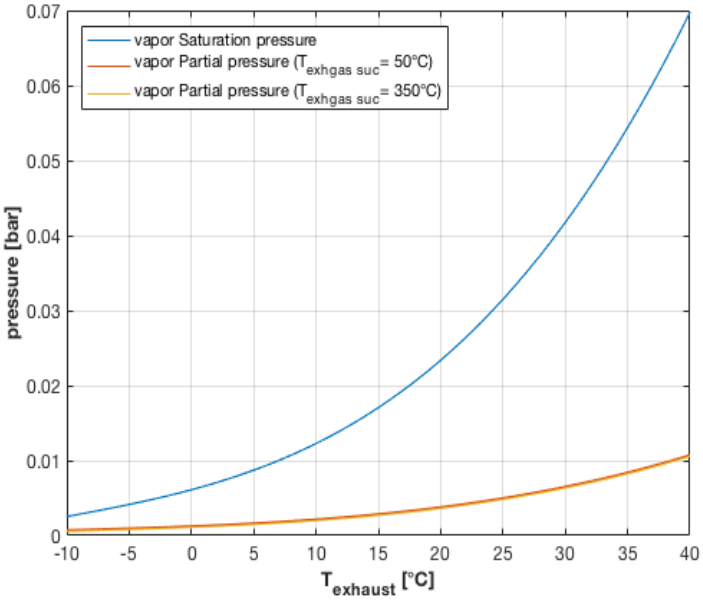

Figure 39. Humidity vs temperature in mix condition

Conclusions and future works

Currently, particulate matter detection is one of the crucial issues of the public and governmental concern in terms of air quality because of the adverse effects on human health and the environment. Among the sources of pollutants, diesel engines are recognized as one of the major sources of PM pollution of the last decades. The verification of the PM emission during vehicle life and the identification of any defect of the after treatment system such as DPF can be achieved through a regular measurement of tailpipe emissions. There exists a wide spectrum of expensive instruments for testing the tailpipe emission in stationary test benches. These professional instruments are very accurate, but due to their high price and bulky structures are not suitable for regular checking of the PM emission after vehicle tailpipe. To address the increasing demand for real-time detection of PM after tailpipe, the design of a compact, low weight, and affordable system including OPC device after tailpipe of the diesel vehicle has been proposed. To fulfill the optical sensor operating requirements, different conditions of the inlet mixture emission, such as relative humidity, concentration and temperature have been considered. Considering the limitation of the particle size detection of the OPC, the accumulated mode of the diesel particulate matter can be considered in the proposed research. However, the accuracy limitation can be improved through a proper calibration and by optimizing the data process [149]. Considering the concentration of the inlet sampling emission of the OPC based on Mie scattering, it is assumed that there is always one particle in the observation sensing at time. To increase the accuracy of the optical detection system, it is necessary to reduce the coincidence error, which occurs if several particles are present in the observation volume simultaneously. For this purpose, one of the solution is to dilute the exhaust emission without any physical changing of the OPC structure. In the present work, the dilution factor of 8 is chosen to decrease the maximum concentration of the exhaust emission to the value of 60 ($\frac{1}{cm^3}$), which decreases the coincidence probability and increases the accuracy of the detection system. To this aim, it has been designed a layout including four ejectors in parallel and one compressor to dilute the emission exhaust gas of the diesel engine tailpipe. In order to use OPC after the proposed layout, different parameters such as partial vapor pressure, humidity, and temperature of the inlet sampling emission before the optical sensor were calculated. The

humidity of the sampled emission before the optical sensor was less than 30%, which is an acceptable range for detection of the particulate matter. The temperature of the mix condition will remain below 45 ℃, which fulfills our requirements. In addition, the sampling flow rate of the inlet was determined in order to guarantee laminar flow conditions in terms of Reynolds number. All these conditions show that using the proposed layout after tailpipe is useful for detecting the particulate matter after diesel engines, especially in terms of faults of DPF, but some efforts are needed to improve the detection range size. The proposed system also needs proper calibration using accurate devices to detect the mass concentration of the particulate matter. In future research, advancements are expected in terms of the detection size by an appropriate calibration and by changing the OPC structures.

References:

[1] "Summary of the Clean Air Act," *US Environmental Protection Agency*. https://www.epa.gov/laws-regulations/summary-clean-air-act (accessed Oct. 01, 2020).

[2] "Criteria Air Pollutants,National Ambient Air Quality Standards (NAAQS)," *US Environmental Protection Agency*. https://www.epa.gov/criteria-air-pollutants (accessed Oct. 01, 2020).

[3] R. D. Brook *et al.*, "Particulate matter air pollution and cardiovascular disease: an update to the scientific statement from the American Heart Association," *Circulation*, vol. 121, no. 21, pp. 2331–2378, 2010.

[4] M. Lacasana, A. Esplugues, and F. Ballester, "Exposure to ambient air pollution and prenatal and early childhood health effects," *Eur. J. Epidemiol.*, vol. 20, no. 2, pp. 183–199, 2005.

[5] P. Klepac, I. Locatelli, S. Korošec, N. Künzli, and A. Kukec, "Ambient air pollution and pregnancy outcomes: A comprehensive review and identification of environmental public health challenges," *Environ. Res.*, vol. 167, pp. 144–159, 2018.

[6] G. Hoek *et al.*, "Long-term air pollution exposure and cardio-respiratory mortality: A review," *Environ. Heal. A Glob. Access Sci. Source*, vol. 12, no. 1, p. 43, Dec. 2013, doi: 10.1186/1476-069X-12-43.

[7] K. Torén, I. A. Bergdahl, T. Nilsson, and B. Järvholm, "Occupational exposure to particulate air pollution and mortality due to ischaemic heart disease and cerebrovascular disease," *Occup. Environ. Med.*, vol. 64, no. 8, pp. 515–519, 2007.

[8] J. O. Anderson, J. G. Thundiyil, and A. Stolbach, "Clearing the air: a

review of the effects of particulate matter air pollution on human health," *J. Med. Toxicol.*, vol. 8, no. 2, pp. 166–175, 2012.

[9] C. I. Davidson, R. F. Phalen, and P. A. Solomon, "Airborne particulate matter and human health: a review," *Aerosol Sci. Technol.*, vol. 39, no. 8, pp. 737–749, 2005.

[10] W. C. Malm, *Fundamentals of Visibility*. John Wiley & Sons Hoboken, NJ, USA, 2003.

[11] "Particulate Matter (PM) Pollution," *United States Environmental Protection Agency*. https://www.epa.gov/pm-pollution (accessed Oct. 02, 2020).

[12] "Particle size fraction definitions for health-related sampling," *International Standardization Organization. ISO 7708:1995 Air quality*. https://www.iso.org/standard/14534.html (accessed Oct. 01, 2020).

[13] "EN 481.Workplace Atmospheres - Size Fraction Definitions for Measurement of Airborne Particles," *European Committee for Standardization*. https://www.cen.eu/Pages/default.aspx (accessed Oct. 01, 2020).

[14] "Revisions to the National Ambient Air Quality Standards for Particulate Matter," *Environmental Protection Agency*, 1987. https://www3.epa.gov/ttn/naaqs/standards/pm/previous/pm-1987-final-52fr24634.pdf.

[15] "Particulate Matter (PM) Pollution," *U.S. Environmental Protection Agency*. https://www.epa.gov/pm-pollution/particulate-matter-pm-basics (accessed Oct. 10, 2020).

[16] "Stationary source emissions -Determination of PM10/PM2,5 mass concentration in flue gas – Measurement at low concentrations by use of impactors," *International Standardization Organization.ISO*

23210:2009. https://www.iso.org/standard/53379.html (accessed Oct. 01, 2020).

[17] G. D. Thurston, "Outdoor air pollution: sources, atmospheric transport, and human health effects," 2017.

[18] M. Park *et al.*, "Differential toxicities of fine particulate matters from various sources," *Sci. Rep.*, vol. 8, no. 1, pp. 1–11, 2018.

[19] P. Kumar *et al.*, "Ultrafine particles in cities," *Environ. Int.*, vol. 66, pp. 1–10, 2014, doi: 10.1016/j.envint.2014.01.013.

[20] "Understanding the Health Effects of Ambient Ultrafine Particles," *Perspectives 3, January 2013*. https://www.healtheffects.org/publication/understanding-health-effects-ambient-ultrafine-particles (accessed Oct. 01, 2020).

[21] G. Oberdörster, E. Oberdörster, and J. Oberdörster, "An emerging discipline evolving from studies of ultrafine particles supplemental web sections," *Environ. Heal. Perspect*, vol. 113, no. 7, pp. 823–839, 2005.

[22] "Diesel Exhaust Particle Size," *DieselNet.com*, 2002. https://dieselnet.com/tech/dpm_size.php (accessed Oct. 10, 2020).

[23] W. Crinnion, "Particulate Matter Is a Surprisingly Common Contributor to Disease," *Integr. Med. A Clin. J.*, vol. 16, no. 4, p. 8, 2017.

[24] K. Donaldson, V. Stone, A. Clouter, L. Renwick, and W. MacNee, "Ultrafine particles," *Occup. Environ. Med.*, vol. 58, no. 3, pp. 211–216, 2001.

[25] M. Harri, P. Svoboda, T. Mori, P. Mutanen, H. Kasai, and K. Savela, "Analysis of 8-hydroxydeoxyguanosine among workers exposed to diesel particulate exhaust: comparison with urinary metabolites and PAH air monitoring," *Free Radic. Res.*, vol. 39, no. 9, pp. 963–972, 2005.

[26] European Environment Agency, “European Union emission inventory report 1990–2013 under the UNECE Convention on Long-range Transboundary Air Pollution (LRTAP).” doi: 10.2800/031449.

[27] F. Karagulian *et al.*, “Contributions to cities’ ambient particulate matter (PM): A systematic review of local source contributions at global level,” *Atmos. Environ.*, vol. 120, pp. 475–483, 2015.

[28] W. Kam, J. W. Liacos, J. J. Schauer, R. J. Delfino, and C. Sioutas, “Size-segregated composition of particulate matter (PM) in major roadways and surface streets,” *Atmos. Environ.*, vol. 55, pp. 90–97, 2012.

[29] A. J. Thorpe, R. M. Harrison, P. G. Boulter, and I. S. McCrae, “Estimation of particle resuspension source strength on a major London Road,” *Atmos. Environ.*, vol. 41, no. 37, pp. 8007–8020, 2007.

[30] W. A. Majewski, “What Are Diesel Emissions,” *DieselNet*, 2012. http://www.dieselnet.com/tech/emi_intro.php (accessed Oct. 01, 2020).

[31] J. B. Heywood, *Combustion engine fundamentals*. 1988.

[32] A. C. Mayer, A. Ulrich, J. Czerwinski, and J. J. Mooney, “Metal-oxide particles in combustion engine exhaust,” SAE Technical Paper, 2010.

[33] S. Steiner, C. Bisig, A. Petri-Fink, and B. Rothen-Rutishauser, “Diesel exhaust: current knowledge of adverse effects and underlying cellular mechanisms,” *Arch. Toxicol.*, vol. 90, no. 7, pp. 1541–1553, 2016.

[34] R. Gligorijevic, J. Jevtic, and G. Biresaw, “The influence of engine oil on diesel exhaust emissions,” *J. Synth. Lubr.*, vol. 21, no. 1, pp. 33–42, 2004.

[35] O. Popovicheva *et al.*, “Diesel/biofuel exhaust particles from modern internal combustion engines: Microstructure, composition, and hygroscopicity,” *Fuel*, vol. 157, pp. 232–239, 2015.

[36] H. Burtscher, “Physical characterization of particulate emissions from diesel engines: a review,” *J. Aerosol Sci.*, vol. 36, no. 7, pp. 896–932, 2005.

[37] İ. A. Reşitoğlu, K. Altinişik, and A. Keskin, “The pollutant emissions from diesel-engine vehicles and exhaust aftertreatment systems,” *Clean Technol. Environ. Policy*, vol. 17, no. 1, pp. 15–27, 2015.

[38] T. Kamimoto and H. Kobayashi, “Combustion processes in diesel engines,” *Prog. Energy Combust. Sci.*, vol. 17, no. 2, pp. 163–189, 1991.

[39] I. A. Reşitoɨlu, K. Altinişik, and A. Keskin, “The pollutant emissions from diesel-engine vehicles and exhaust aftertreatment systems,” *Clean Technologies and Environmental Policy*, vol. 17, no. 1. Springer Verlag, pp. 15–27, Jan. 04, 2015, doi: 10.1007/s10098-014-0793-9.

[40] R. B. G. A. A. S. M. A. D. D. AA/MKA5 and T. Raatz, *Emissions-control technology for diesel engines*. Robert Bosch GmbH, Automotive Equipment Business Sector, Department for …, 2005.

[41] Z. D. Ristovski *et al.*, “Respiratory health effects of diesel particulate matter,” *Respirology*, vol. 17, no. 2, pp. 201–212, 2012.

[42] D. B. Kittelson, “Engines and nanoparticles: a review,” *J. Aerosol Sci.*, vol. 29, no. 5–6, pp. 575–588, 1998.

[43] D. A. Morgott, “Factors and trends affecting the identification of a reliable biomarker for diesel exhaust exposure,” *Crit. Rev. Environ. Sci. Technol.*, vol. 44, no. 16, pp. 1795–1864, 2014.

[44] S. Mohankumar and P. Senthilkumar, “Particulate matter formation and its control methodologies for diesel engine: A comprehensive review,” *Renew. Sustain. Energy Rev.*, vol. 80, pp. 1227–1238, 2017.

[45] M. D. Geller *et al.*, “Physicochemical and redox characteristics of

particulate matter (PM) emitted from gasoline and diesel passenger cars," *Atmos. Environ.*, vol. 40, no. 36, pp. 6988–7004, 2006, doi: 10.1016/j.atmosenv.2006.06.018.

[46] D. Fino, "Diesel emission control: Catalytic filters for particulate removal," *Sci. Technol. Adv. Mater.*, vol. 8, no. 1–2, pp. 93–100, 2007.

[47] H. Burtscher and W. A. Majewski, "Particulate Matter Measurements," *DieselNet*, 2012. https://www.dieselnet.com/tech/measure_dpm.php (accessed Oct. 01, 2020).

[48] K. Yang, J. T. Fox, and R. Hunsicker, "Characterizing diesel particulate filter failure during commercial fleet use due to pinholes, melting, cracking, and fouling," *Emiss. Control Sci. Technol.*, vol. 2, no. 3, pp. 145–155, 2016.

[49] J. S. Lighty, J. M. Veranth, and A. F. Sarofim, "Combustion aerosols: factors governing their size and composition and implications to human health," *J. Air Waste Manage. Assoc.*, vol. 50, no. 9, pp. 1565–1618, 2000.

[50] F. Wikipedia, "European emission standards," 2014. https://en.wikipedia.org/wiki/European_emission_standards (accessed Oct. 01, 2020).

[51] "Emission standards,EU: Cars and Light Trucks," *DieselNet*. https://dieselnet.com/standards/eu/ld.php (accessed Oct. 10, 2020).

[52] H. Al-Thani, M. Koç, C. Fountoukis, and R. J. Isaifan, "Evaluation of particulate matter emissions from non-passenger diesel vehicles in Qatar," *J. Air Waste Manage. Assoc.*, vol. 70, no. 2, pp. 228–242, 2020.

[53] B. Giechaskiel *et al.*, "Review of motor vehicle particulate emissions sampling and measurement: From smoke and filter mass to particle number," *J. Aerosol Sci.*, vol. 67, pp. 48–86, Jan. 2014, doi:

10.1016/j.jaerosci.2013.09.003.

[54] T. Nussbaumer, C. Czasch, N. Klippel, L. Johansson, and C. Tullin, "Particulate emissions from biomass combustion in IEA countries," *16th Eur. biomass Conf. Exhib.*, vol. 32, no. January, p. 40, 2008, doi: http://www.ieabcc.nl/publications/Nussbaumer_et_al_IEA_Report_PM10_Jan_2008.pdf.

[55] D. L. Hofeldt, "Real-time soot concentration measurement technique for engine exhaust streams," SAE Technical Paper, 1993.

[56] C. F. Bohren and D. R. Huffman, "Book-Review-Absorption and Scattering of Light by Small Particles," *Natur*, vol. 307, p. 575, 1984.

[57] A. Pillarisetti *et al.*, "Small, Smart, Fast, and Cheap: Microchip-Based Sensors to Estimate Air Pollution Exposures in Rural Households," *Sensors*, vol. 17, no. 8, p. 1879, Aug. 2017, doi: 10.3390/s17081879.

[58] "keison product;TSI dust-Areosol monitor." https://www.keison.co.uk/tsi-dust-monitors.shtml?gclid=CjwKCAjwn9v7BRBqEiwAbq1Ey-Swlt3eKeQAzJP5I22nFl9smUeBU7b-N1H5567vI3naNIfByWD4aBoCGLYQAvD_BwE (accessed Oct. 01, 2020).

[59] F. T. Gucker, C. T. O'Konski, H. B. Pickard, and J. N. Pitts, "A Photoelectronic Counter for Colloidal Particles," *J. Am. Chem. Soc.*, vol. 69, no. 10, pp. 2422–2431, Oct. 1947, doi: 10.1021/ja01202a053.

[60] B. Y. H. Liu, R. N. Berglund, and J. K. Agarwal, "Experimental studies of optical particle counters," *Atmos. Environ.*, vol. 8, no. 7, pp. 717–732, 1974.

[61] P. Kulkarni, P. A. Baron, and K. Willeke, *Aerosol measurement: principles, techniques, and applications*. John Wiley & Sons, 2011.

[62] W. Zhao, W. Tan, G. Zhao, C. Shen, Y. Yu, and C. Zhao, "Determination of black carbon mass concentration from aerosol light absorption using variable mass absorption cross-section," *Atmos. Meas. Tech. Discuss.*, pp. 1–17, 2020.

[63] "Reliable and robust measuring equipment;AVL smok meter." .

[64] C. Liousse, H. Cachier, and S. G. Jennings, "Optical and thermal measurements of black carbon aerosol content in different environments: Variation of the specific attenuation cross-section, sigma (σ)," *Atmos. Environ. Part A. Gen. Top.*, vol. 27, no. 8, pp. 1203–1211, 1993.

[65] A. Petzold and R. Niessner, "Photoacoustic soot sensor for in-situ black carbon monitoring," *Appl. Phys. B Laser Opt.*, vol. 63, no. 2, pp. 191–197, Aug. 1996, doi: 10.1007/BF01095272.

[66] W. Schindler, C. Haisch, H. A. Beck, R. Niessner, E. Jacob, and D. Rothe, "A photoacoustic sensor system for time resolved quantification of diesel soot emissions," *SAE Tech. Pap.*, pp. 483–490, 2004, doi: 10.4271/2004-01-0968.

[67] AVL, "Avl Micro Soot Sensor," 2011. https://www.avl.com/-/mssplus-avl-micro-soot-sensor (accessed Oct. 01, 2020).

[68] N. Moteki and Y. Kondo, "Dependence of laser-induced incandescence on physical properties of black carbon aerosols: Measurements and theoretical interpretation," *Aerosol Sci. Technol.*, vol. 44, no. 8, pp. 663–675, 2010.

[69] P. J. Groblicki and C. R. Begeman, "Particle Size Variation in Diesel Car Exhaust," Feb. 1979, doi: 10.4271/790421.

[70] H. J. W. Addy Majewski, "DieselNet; Smok Opacity." https://dieselnet.com/tech/measure_opacity.php (accessed Oct. 01,

2020).

[71] F. R. Faxvog and D. M. Roessler, “Mass concentration of diesel particle emissions from photoacoustic and opacity measurements,” *Aerosol Sci. Technol.*, vol. 1, no. 2, pp. 225–234, 1982, doi: 10.1080/02786828208958590.

[72] H. Patashnick and E. G. Rupprecht, “Continuous PM-10 measurements using the tapered element oscillating microbalance,” *J. Air Waste Manage. Assoc.*, vol. 41, no. 8, pp. 1079–1083, 1991.

[73] P. O. Witze, R. E. Chase, M. M. Maricq, D. H. Podsiadlik, and N. Xu, “Time-resolved measurements of exhaust PM for FTP-75: Comparison of LII, ELPI, and TEOM Techniques,” SAE Technical Paper, 2004.

[74] D. R. Booker, R. A. Giannelli, and J. Hu, “Road test of an on-board particulate matter mass measurement system,” SAE Technical Paper, 2007.

[75] D. P. Poenar, “Microfluidic and micromachined/MEMS devices for separation, discrimination and detection of airborne particles for pollution monitoring,” *Micromachines*, vol. 10, no. 7, p. 483, 2019.

[76] I. Paprotny, F. Doering, P. A. Solomon, R. M. White, and L. A. Gundel, “Microfabricated air-microfluidic sensor for personal monitoring of airborne particulate matter: Design, fabrication, and experimental results,” *Sensors Actuators A Phys.*, vol. 201, pp. 506–516, 2013.

[77] J. Liu, W. Hao, M. Liu, Y. Liang, and S. He, “A novel particulate matter 2.5 sensor based on surface acoustic wave technology,” *Appl. Sci.*, vol. 8, no. 1, p. 82, 2018.

[78] A. Rostedt *et al.*, “Non-collecting electrical sensor for particle concentration measurement,” *Aerosol Air Qual. Res.*, vol. 9, no. 4, pp. 470–477, 2009.

[79] L. Ntziachristos, P. Fragkiadoulakis, Z. Samaras, K. Janka, and J. Tikkanen, “Exhaust particle sensor for OBD application,” SAE Technical Paper, 2011.

[80] E. Papaioannou *et al.*, “The SUREAL-23 project: Understanding and Measuring Sub-23 nm Particle Emissions from Direct Injection Engines,” *Earpa.Eu*, p. 41, 2018, [Online]. Available: https://www.earpa.eu/ENGINE/FILES/EARPA/WEBSITE/UPLOAD/FILE/formforum/presentations/papers_invited_speakers_and_yr/sp01ff2018_papaioannou_the_sureal_23_project.pdf.

[81] J. H. Vincent, *Aerosol sampling: science, standards, instrumentation and applications*. John Wiley & Sons, 2007.

[82] M. Wentzel, H. Gorzawski, K.-H. Naumann, H. Saathoff, and S. Weinbruch, “Transmission electron microscopical and aerosol dynamical characterization of soot aerosols,” *J. Aerosol Sci.*, vol. 34, no. 10, pp. 1347–1370, 2003.

[83] K. Park, D. B. Kittelson, and P. H. McMurry, “Structural properties of diesel exhaust particles measured by transmission electron microscopy (TEM): Relationships to particle mass and mobility,” *Aerosol Sci. Technol.*, vol. 38, no. 9, pp. 881–889, 2004.

[84] J. Song, M. Alam, A. L. Boehman, and U. Kim, “Examination of the oxidation behavior of biodiesel soot,” *Combust. Flame*, vol. 146, no. 4, pp. 589–604, 2006.

[85] W. C. Hinds, *Aerosol technology: properties, behavior, and measurement of airborne particles*. John Wiley & Sons, 1999.

[86] J. Keskinen, K. Pietarinen, and M. Lehtimäki, “Electrical low pressure impactor,” *J. Aerosol Sci.*, vol. 23, no. 4, pp. 353–360, 1992, doi: 10.1016/0021-8502(92)90004-F.

[87] M. Fierz, L. Scherrer, and H. Burtscher, “Real-time measurement of aerosol size distributions with an electrical diffusion battery,” *J. Aerosol Sci.*, vol. 33, no. 7, pp. 1049–1060, 2002.

[88] M. Fierz, S. Weimer, and H. Burtscher, “Design and performance of an optimized electrical diffusion battery,” *J. Aerosol Sci.*, vol. 40, no. 2, pp. 152–163, Feb. 2009, doi: 10.1016/j.jaerosci.2008.09.007.

[89] R. C. Flagan, “History of electrical aerosol measurements,” *Aerosol Sci. Technol.*, vol. 28, no. 4, pp. 301–380, 1998.

[90] P. Intra and N. Tippayawong, “An overview of differential mobility analyzers for size classification of nanometer-sized aerosol particles.,” *Songklanakarin J. Sci. Technol.*, vol. 30, no. 2, 2008.

[91] K. Reavell, T. Hands, and N. Collings, “A fast response particulate spectrometer for combustion aerosols,” *SAE Trans.*, pp. 1338–1344, 2002.

[92] S. Manual, “Engine exhaust particle sizer™ (eeps™) spectrometer model 3090/3090ak,” 2015. https://www.luchsinger.it/contents/products/data_sheet_particle_sizer_3090-5B1-5D.pdf (accessed Oct. 20, 2020).

[93] J. P. R. Symonds, K. S. J. Reavell, J. S. Olfert, B. W. Campbell, and S. J. Swift, “Diesel soot mass calculation in real-time with a differential mobility spectrometer,” *J. Aerosol Sci.*, vol. 38, no. 1, pp. 52–68, 2007, doi: 10.1016/j.jaerosci.2006.10.001.

[94] E. Zervas *et al.*, “Comparison between the exhaust particles mass determined by the European regulatory gravimetric method and the mass estimated by ELPI,” *SAE Trans.*, pp. 927–943, 2005.

[95] “Dekati ELPI+ Electrical Low Pressure Impactor.” https://www.dekati.com/wp-content/uploads/elpiplus-brochure-

062018.pdf (accessed Oct. 02, 2020).

[96] J. S. Olfert and N. Collings, “New method for particle mass classification—the Couette centrifugal particle mass analyzer,” *J. Aerosol Sci.*, vol. 36, no. 11, pp. 1338–1352, 2005.

[97] “New Periodic Technical Inspections (NPTI).” https://dieselnet.com/standards/eu/pti.php (accessed Nov. 10, 2020).

[98] “CONDENSATION PARTICLE COUNTERS.” https://tsi.com/products/particle-counters-and-detectors/condensation-particle-counters (accessed Oct. 01, 2020).

[99] “PARTICLE NUMBER MEASUREMENT.” http://www.sensors-inc.com/Products/SEMTECH/CPN (accessed Nov. 01, 2020).

[100] O. Spiel Vogel, Jureng. BischofI, Oliver F. Franken and D. Booker, “Challenges of intriducting PN-PTI in Germany and other countries.” https://www.tsi.com/getmedia/6d52f6f2-5a37-481a-9c68-8ec05f0a5906/White-Paper_PI_PTI_Feb-2020_A4_Web (accessed Oct. 02, 2020).

[101] M. Budde, P. Barbera, R. El Masri, T. Riedel, and M. Beigl, “Retrofitting smartphones to be used as particulate matter dosimeters,” Sep. 2013, p. 139, doi: 10.1145/2493988.2494342.

[102] M. Budde, M. Köpke, and M. Beigl, “Design of a light-scattering particle sensor for citizen science air quality monitoring with smartphones: Tradeoffs and experiences,” 2016, doi: 10.14644/dust.2016.003.

[103] M. Budde, S. Leiner, M. Köpke, J. Riesterer, T. Riedel, and M. Beigl, “Feinphone: Low-cost smartphone camera-based 2D particulate matter sensor,” *Sensors (Switzerland)*, vol. 19, no. 3, Feb. 2019, doi: 10.3390/s19030749.

[104] Y. Qiao *et al.*, “Sub-micro Particle Matter Detection for Metal Three Dimensional Printing Workshop,” *IEEE Sens. J.*, pp. 1–1, Feb. 2019, doi: 10.1109/jsen.2019.2902223.

[105] “WHO Air quality guidelines for particulate matter, ozone, nitrogen dioxide and sulfur dioxide.Global update 2005.” https://apps.who.int/iris/bitstream/handle/10665/69477/WHO_SDE_PHE_OEH_06.02_eng.pdf?sequen%0Dce=1 (accessed Oct. 02, 2020).

[106] X. Li *et al.*, “Miniaturized particulate matter sensor for portable air quality monitoring devices,” in *SENSORS, 2014 IEEE*, 2014, pp. 2151–2154.

[107] M. Dong, E. Iervolino, F. Santagata, G. Zhang, and G. Zhang, “Integrated virtual impactor enabled PM 2.5 sensor,” *IEEE Sens. J.*, vol. 17, no. 9, pp. 2814–2821, 2017.

[108] M. Dong, E. Iervolino, F. Santagata, G. Zhang, and G. Zhang, “Silicon microfabrication based particulate matter sensor,” *Sensors Actuators, A Phys.*, vol. 247, pp. 115–124, Aug. 2016, doi: 10.1016/j.sna.2016.05.036.

[109] R. Schrobenhauser, R. Strzoda, A. Hartmann, M. Fleischer, and M.-C. Amann, “Miniaturized sensor for particles in air using Fresnel ring lenses and an enhanced intensity ratio technique,” *Appl. Opt.*, vol. 53, no. 4, pp. 625–633, 2014.

[110] R. Schrobenhauser, R. Strzoda, M. Fleischer, A. Hartmann, and M.-C. Amann, “Detection of the mass of fine particulate matter using light scattering and inertial filtering in a miniaturized sensor setup,” *Meas. Sci. Technol.*, vol. 25, no. 3, p. 035103, Mar. 2014, doi: 10.1088/0957-0233/25/3/035103.

[111] R. S. Gao *et al.*, “A high-sensitivity low-cost optical particle counter

design," *Aerosol Sci. Technol.*, vol. 47, no. 2, pp. 137–145, Feb. 2013, doi: 10.1080/02786826.2012.733039.

[112] L. Lombardo, M. Parvis, E. Angelini, and S. Grassini, "An Optical Sampling System for Distributed Atmospheric Particulate Matter," *IEEE Trans. Instrum. Meas.*, pp. 1–8, Jan. 2019, doi: 10.1109/tim.2019.2890885.

[113] L. Lombardo, M. Parvis, E. Angelini, and S. Grassini, "Optical solution for particulate distribution estimation," in *I2MTC 2018 - 2018 IEEE International Instrumentation and Measurement Technology Conference: Discovering New Horizons in Instrumentation and Measurement, Proceedings*, Jul. 2018, pp. 1–6, doi: 10.1109/I2MTC.2018.8409749.

[114] G. S. Lombardo Luca, Parvis Marco, Vitiello Francesco, Angelini Emma, "A Sensor Network for Particulate Distribution Estimation," *IEEE, Int. Symp. Med. Meas. Appl. (MeMeA), Rome*, pp. 1–6, 2018.

[115] A. Proietti, M. Panella, F. Leccese, and E. Svezia, "Dust detection and analysis in museum environment based on pattern recognition," *Meas. J. Int. Meas. Confed.*, vol. 66, pp. 62–72, 2015, doi: 10.1016/j.measurement.2015.01.019.

[116] A. Proietti, F. Leccese, M. Caciotta, F. Morresi, U. Santamaria, and C. Malomo, "A new dusts sensor for cultural heritage applications based on image processing," *Sensors*, vol. 14, no. 6, pp. 9813–9832, 2014.

[117] G. Brunnhofer, A. Bergmann, and M. Kraft, "Concept for a holographic particle counter," in *30th Annual Conference of the IEEE Photonics Society, IPC 2017*, Nov. 2017, vol. 2017-Janua, pp. 581–582, doi: 10.1109/IPCon.2017.8116233.

[118] G. Brunnhofer, A. Bergmann, A. Klug, and M. Kraft, "Design and

validation of a holographic particle counter," *Sensors*, vol. 19, no. 22, p. 4899, 2019.

[119] G. Brunnhofer and A. Bergmann, "Modelling a Holographic Particle Counter," *Proceedings*, vol. 2, no. 13, p. 967, Nov. 2018, doi: 10.3390/proceedings2130967.

[120] B. Sachweh, H. Umhauer, F. Ebert, H. Büttner, and R. Friehmelt, "In situ optical particle counter with improved coincidence error correction for number concentrations up to 107 particles cm−3," *J. Aerosol Sci.*, vol. 29, no. 9, pp. 1075–1086, Oct. 1998, doi: 10.1016/S0021-8502(98)80004-9.

[121] D. J. Kerbyson and T. J. Atherton, "Circle detection using Hough transform filters," 1995.

[122] X. Li, L. Xie, and X. Zheng, "The comparison between the Mie theory and the Rayleigh approximation to calculate the EM scattering by partially charged sand," *J. Quant. Spectrosc. Radiat. Transf.*, vol. 113, no. 3, pp. 251–258, 2012.

[123] F. T. Gucker Jr, C. T. O'Konski, H. B. Pickard, and J. N. Pitts Jr, "A photoelectronic counter for colloidal particles1," *J. Am. Chem. Soc.*, vol. 69, no. 10, pp. 2422–2431, 1947.

[124] S. Molaei, "The measurement of Young's modulus of thin films using secondary laser speckle patterns," *Measurement*, vol. 92, pp. 28–33, 2016.

[125] A. C. Eriksson *et al.*, "Diesel soot aging in urban plumes within hours under cold dark and humid conditions," *Sci. Rep.*, vol. 7, no. 1, pp. 1–10, 2017.

[126] P. D. Rosenberg *et al.*, "Particle sizing calibration with refractive index correction for light scattering optical particle counters and impacts upon

PCASP and CDP data collected during the Fennec campaign," *Atmos. Meas. Tech.*, vol. 5, no. 5, pp. 1147–1163, 2012, doi: 10.5194/amt-5-1147-2012.

[127] M. Budde, M. Busse, and M. Beigl, "Investigating the use of commodity dust sensors for the embedded measurement of particulate matter," in *2012 Ninth International Conference on Networked Sensing (INSS)*, Jun. 2012, pp. 1–4, doi: 10.1109/INSS.2012.6240545.

[128] S. Sousan, K. Koehler, L. Hallett, and T. M. Peters, "Evaluation of the Alphasense optical particle counter (OPC-N2) and the Grimm portable aerosol spectrometer (PAS-1.108)," *Aerosol Sci. Technol.*, vol. 50, no. 12, pp. 1352–1365, Dec. 2016, doi: 10.1080/02786826.2016.1232859.

[129] H. Grimm and D. J. Eatough, "Aerosol measurement: the use of optical light scattering for the determination of particulate size distribution, and particulate mass, including the semi-volatile fraction," *J. Air Waste Manage. Assoc.*, vol. 59, no. 1, pp. 101–107, 2009.

[130] J. Raasch and H. Umhauer, "Errors in the Determination of Particle Size Distributions Caused by Coincidences in Optical Particle Counters," 1984.

[131] K. T. Whitby and K. Willeke, "Single particle optical counters: principles and field use," *Aerosol Meas.*, pp. 145–182, 1979.

[132] J. Raasch and H. Umhauer, "Errors in the Determination of Particle Size Distributions Caused by coincidences in optical particle counters," 1984. doi: 10.1002/ppsc.19840010109.

[133] B. E. Rapp, *Microfluidics: modeling, mechanics and mathematics*. William Andrew, 2016.

[134] M. Ott, "Capabilities and reliability of LEDs and laser diodes," *Intern. NASA Parts Packag. Publ.*, 1996.

[135] R. Jayaratne, X. Liu, P. Thai, M. Dunbabin, and L. Morawska, “The influence of humidity on the performance of a low-cost air particle mass sensor and the effect of atmospheric fog,” *Atmos. Meas. Tech.*, vol. 11, no. 8, pp. 4883–4890, Aug. 2018, doi: 10.5194/amt-11-4883-2018.

[136] L. R. Crilley *et al.*, “Evaluation of a low-cost optical particle counter (Alphasense OPC-N2) for ambient air monitoring,” *Atmos. Meas. Tech. Discuss.*, pp. 1–24, Aug. 2017, doi: 10.5194/amt-2017-308.

[137] A. Di Antonio, O. A. M. Popoola, B. Ouyang, J. Saffell, and R. L. Jones, “Developing a relative humidity correction for low-cost sensors measuring ambient particulate matter,” *Sensors (Switzerland)*, vol. 18, no. 9, Sep. 2018, doi: 10.3390/s18092790.

[138] M. Badura, P. Batog, A. Drzeniecka-Osiadacz, and P. Modzel, “Evaluation of low-cost sensors for ambient PM2.5 monitoring,” *J. Sensors*, vol. 2018, 2018, doi: 10.1155/2018/5096540.

[139] D. Wang, Z. C. Liu, J. Tian, J. W. Liu, and J. R. Zhang, “Investigation of particle emission characteristics from a diesel engine with a diesel particulate filter for alternative fuels,” *Int. J. Automot. Technol.*, vol. 13, no. 7, pp. 1023–1032, 2012, doi: 10.1007/s12239−012−0105−5.

[140] “OPC-N3 particle monitor for use in high pollution urban environments, Technical specification.” http://www.alphasense.com/WEB1213/wp-content/uploads/2019/03/OPC-N3.pdf (accessed Aug. 18, 2020).

[141] “GRIMM AEROSOL.” https://www.grimm-aerosol.com/ (accessed Nov. 01, 2020).

[142] “Laboratory evaluation AlphaSense OPC-N3 sensor.” http://www.aqmd.gov/docs/default-source/aq-spec/laboratory-evaluations/alphasense-opc-n3---lab-evaluation.pdf?sfvrsn=14 (accessed Oct. 01, 2020).

[143] "Particulate Matter Measurements." https://dieselnet.com/tech/measure_dpm.php (accessed Oct. 02, 2020).

[144] A. Rostedt *et al.*, "A new miniaturized sensor for ultra-fast on-board soot concentration measurements," *SAE Int. J. Engines*, vol. 10, no. 4, pp. 1859–1865, 2017.

[145] A. D. Melas *et al.*, "Development and evaluation of a catalytic stripper for the measurement of solid ultrafine particle emissions from internal combustion engines," *Aerosol Sci. Technol.*, vol. 54, no. 6, pp. 704–717, 2020.

[146] "Body ported Type Vacuum Ejector, Z. S.,." https://docs.rs-online.com/8a2f/0900766b81662bda.pdf (accessed Oct. 02, 2020).

[147] L. Jing, "Standard Combustion Aerosol Generator (SCAG) for Calibration Purposes," in *Atmospheric Environment*, 1999, vol. 27, no. 8, pp. 1271–1275.

[148] R. Jayaratne, X. Liu, P. Thai, M. Dunbabin, and L. Morawska, "The influence of humidity on the performance of a low-cost air particle mass sensor and the effect of atmospheric fog," *Atmos. Meas. Tech.*, vol. 11, no. 8, pp. 4883–4890, Aug. 2018, doi: 10.5194/amt-11-4883-2018.

[149] M. Budde, R. El Masri, T. Riedel, and M. Beigl, "Enabling low-cost particulate matter measurement for participatory sensing scenarios," in *Proceedings of the 12th International Conference on Mobile and Ubiquitous Multimedia - MUM '13*, 2013, pp. 1–10, doi: 10.1145/2541831.2541859.